MOOSE's PorousFlow module: verification tests

Andy Wilkins and Chris Green

CSIRO

March 30, 2017

Abstract

This document describes the physics captured by MOOSE's PorousFlow module, as well as describing various numerical aspects and tips to ensure good convergence.

Each nontrivial test in the test suite *has its own separate documentation* and these should help users understand more clearly how to build a PorousFlow input file.

Within this document, black text indicates funcionality that has been implemented and tested and red text indicates functionality that should be implemented by December 2017.

Contents

Chapter 1

PorousFlowFluidMass postprocessor

1.1   Single-phase, single-component

The total fluid mass of species sp within a volume V is

$$\int_V \phi \sum_{\mathrm{ph}} \rho_{\mathrm{ph}} S_{\mathrm{ph}} \chi_{\mathrm{ph}}^{\mathrm{sp}} \; . \tag{1.1}$$

It must be checked that MOOSE calculates this correctly in order that mass-balances be correct, and also because this quantity is used in a number of other tests

A 1D model with $-1 \leq x \leq 1$, and with three elements of size 1 is created with the following properties:

Constant fluid bulk modulus	$1\,\mathrm{Pa}$
Fluid density at zero pressure	$1\,\mathrm{kg.m}^{-3}$
Van Genuchten m	0.5
Van Genuchten α	$1\,\mathrm{Pa}^{-1}$
Porosity	0.1

The porepressure is set at $P = x$.

Recall that in PorousFlow, mass is lumped to the nodes. Therefore, the integral above is evaluated at the nodes, and a sum of the results is outputted as the PorousFlowFluidMass postprocessor. Using the properties given above, this yields:

x	p	Density	Saturation	Nodal mass
-1	-1	0.367879441	0.707106781	0.008671002
-0.333333333	-0.333333333	0.716531311	0.948683298	0.02265871
-0.333333333	-0.333333333	0.716531311	0.948683298	0.02265871
0.333333333	0.333333333	1.395612425	1	0.046520414
0.333333333	0.333333333	1.395612425	1	0.046520414
1	1	2.718281828	1	0.090609394
			Total	0.237638643

MOOSE also gives the total mass as 0.237638643 kg. This test is part of the automatic test suite that is run every time the code is updated.

1.2 Single-phase, two-components

The same test as Section 6.2 is run but with two components. The mass fraction is fixed at

$$\chi_{\mathrm{ph}=0}^{\mathrm{sp}=0} = x^2 \ . \tag{1.2}$$

x	p	Density	Saturation	$\chi_{\mathrm{ph}=0}^{\mathrm{sp}=0}$	Nodal mass$_{\mathrm{sp}=0}$	Nodal mass$_{\mathrm{sp}=1}$
-1	-1	0.367879441	0.707106781	1	0.008671	0
-0.333333333	-0.333333333	0.716531311	0.948683298	0.111111	0.00251763	0.02014108
-0.333333333	-0.333333333	0.716531311	0.948683298	0.111111	0.00251763	0.02014108
0.333333333	0.333333333	1.395612425	1	0.111111	0.00516893	0.04135148
0.333333333	0.333333333	1.395612425	1	0.111111	0.00516893	0.04135148
1	1	2.718281828	1	1	0.09060939	0
				Total	0.11465353	0.12298511

MOOSE produces the expected answer.

1.3 Two-phase, two-components

A 1D model with two elements from $0 \le x \le 1$ is created, with two phases (0 and 1), and two fluid components (0 and 1). The phase densities are calculated using a constant bulk modulus fluid with bulk modulus of 1 Pa. The density at zero pressure is 1 kg m-3 for phase 0, and 0.1 kg m^{-3} for phase 1. The porepressure of phase 0 is held fixed at 1 Pa, and a constant capillary pressure of 0 is specified so that the pressure of phase 1 is also 1 Pa. This results in phase densities of $e = 2.71812818...$ kg m^{-3} for phase 0, and $0.271812818...$ kg m^{-3} for phase 1.

Saturation of phase 1 varies linearly as $1 - x$, while porosity is 0.1 throughout. The mass fraction of species 0 in fluid phase 0 is specified as 0.3, while the mass fraction of species 0 in phase 1 is 0.55. It is simple to calculate the total mass of each component in each phase using Eq. (1.1), the results of which are

Species	Phase	Total mass (Eq. (1.1))	Total mass (MOOSE)
0	0	0.04077423	0.04077423
0	1	0.007475275	0.007475275
0	all	0.04824950	0.04824950
1	0	0.09513986	0.09513986
1	1	0.006116134	0.006116134
1	all	0.10125560	0.1012560

Chapter 2

Jacobian Tests

2.1   Fluid-mass time derivative

The following tests of the Jacobian are performed on the fluid-mass time derivative kernel (PorousFlowMassTimeDerivative).

1. single-phase, with a single component, with a van-Genuchten capillary pressure, constant bulk-modulus density and constant porosity.

2. single-phase, with 3 components, with a van-Genuchten capillary pressure, constant bulk-modulus density and constant porosity.

3. 2-phase PP formulation, with 2 components (that exist in both phases), with a van-Genuchten capillary pressure, constant bulk-modulus density for each phase and constant porosity.

4. 2-phase PP formulation, with 3 components (that exist in both phases), with a van-Genuchten capillary pressure, constant bulk-modulus density for each phase and constant porosity.

2.2   Fluid Advective Flux

The following tests of the Jacobian are performed on the fluid-mass advective flux kernel (PorousFlowAdvectiveFlux).

1. single-phase, with 1 component, constant viscosity, constant insitu-permeability, density with constant bulk modulus, Corey relative permeability, nonzero gravity, with van-Genuchten capillary pressure.

2. single-phase, with 3 components, constant viscosity, constant insitu-permeability, density with constant bulk modulus, Corey relative permeability, nonzero gravity, with van-Genuchten capillary pressure.

3. 2-phase (PP formulation), with 2 components (that exist in both phases), constant viscosity for each phase, constant insitu-permeability, density with constant bulk modulus for each phase, Corey relative permeability for each phase, nonzero gravity, with van-Genuchten capillary pressure.

4. 2-phase (PP formulation), with 3 components (that exist in both phases), constant viscosity for each phase, constant insitu-permeability, density with constant bulk modulus for each phase, Corey relative permeability for each phase, nonzero gravity, with van-Genuchten capillary pressure.

Chapter 3

Dirac kernels

3.1   Geometric tests

The test suite contains tests that demonstrate:

- when a point sink is placed at a node, it withdraws fluid (or heat) from only that node;

- when a point sink that is proportional to mobility (or relative permeability, etc) is placed in an element where some nodes have zero mobility (or relative permeability, etc), then fluid (or heat) is not extracted from those nodes.

3.2   Peaceman borehole fluxes

The automatic test suite contains four tests that check that the Peaceman flux

$$f(P_i, x_i) = W \left| C(P_i - P_{\text{bh}}) \right| \frac{k_{\text{r}}\rho}{\mu}(P_i - P_{\text{bh}}) \tag{3.1}$$

is correctly implemented. A vertical borehole is placed through the centre of a single element, and fluid flow to the borehole as a function of porepressure is measured. The tests are

- A production borehole with $P_{\text{bh}} = 0$, with a fully-saturated medium.

- An injection borehole with $P_{\text{bh}} = 10\,\text{MPa}$, with a fully-saturated medium.

- A production borehole with $P_{\text{bh}} = -1\,\text{MPa}$, with an unsaturated medium.

- An injection borehole with $P_{\text{bh}} = 0$, with an unsaturated medium.

The parameters common to these tests are:

Element size	$2 \times 2 \times 2\,\mathrm{m}^3$
Borehole radius	$0.1\,\mathrm{m}$
Permeability	$10^{-12}\,\mathrm{m}^2$
Gravity	0
Unit fluid weight	0
Fluid reference density	$1000\,\mathrm{kg.m}^{-3}$
Fluid bulk modulus	$2\,\mathrm{GPa}$
Fluid viscosity	$10^{-3}\,\mathrm{Pa.s}$
Van Genuchten α	$10^{-5}\,\mathrm{Pa}$
Van Genuchten m	0.8
Residual saturation	0
FLAC relperm m	2

It is remotely possible that the MOOSE implementation *applies* the borehole flux incorrectly, but *records* it as a Postprocessor correctly as specified by Eqn (3.1). Therefore, these four simulations also record the fluid mass and mass-balance error in order to check that the fluid mass is indeed being correctly changed by the borehole. Figure 3.1 demonstrates that Eqn (3.1) is indeed correctly implemented in MOOSE.

3.3 Comparison with analytic solution

The Richards' equation for a fully-saturated medium with $\rho \propto \exp(P/B)$ and large constant bulk modulus B becomes Darcy's equation

$$\frac{\partial}{\partial t}\rho = \nabla_i \alpha_{ij} \nabla_j \rho \tag{3.2}$$

where $\alpha_{ij} = k_{ij}B/(\mu\phi)$, with notation described in the Theory Manual. In the isotropic case (where $k_{ij} = \kappa\delta_{ij}$), the steadystate equation is just Laplace's equation

$$\nabla^2 \rho = 0 \ , \tag{3.3}$$

Place a borehole of radius r_{bh} and infinite length oriented along the z axis. Then the situation becomes 2D and can be solved in cylindrical coordinates, with $\rho = \rho(r, \theta)$ and independent of z. If the pressure at the borehole wall $r = r_{\mathrm{bh}}$ is P_{bh}, then the fluid density is $\rho_{\mathrm{bh}} \propto \exp(P_{\mathrm{bh}}/B)$. Assume that at $r = R$ the fluid pressure is held fixed at P_R, or equivalently the density is held fixed at ρ_R. Then the solution of Laplace's equation is well-known to be

$$\rho = \rho_{\mathrm{bh}} + (\rho_R - \rho_{\mathrm{bh}})\frac{\log(r/r_{\mathrm{bh}})}{\log(R/r_{\mathrm{bh}})} \ . \tag{3.4}$$

This is the fundamental solution used by Peaceman and others to derive expressions for W by comparing with numerical expressions resulting from Eqn (3.1) (see Theory Manual for more details).

Chen and Zhang (see Theory manual) have derived an expression for W in the case where this borehole is placed at a node in a square mesh. This test compares the MOOSE steadystate solution with a single borehole with W defined by Chen and Zhang's formula is compared with Eqn (3.4) to illustrate that the MOOSE implementation of a borehole is correct.

Figure 3.3 shows this comparison. Most parameters in this study are identical to those given in the above table with the following exceptions: the mesh is shown in Fig 3.2; the permeability is $10^{-11}\,\mathrm{m}^2$; the borehole radius is $1\,\mathrm{m}$; the borehole pressure is $P_{\mathrm{bh}} = 0$; the outer radius is $r = 300\,\mathrm{m}$; and the outer pressure is $P_R = 10\,\mathrm{MPa}$.
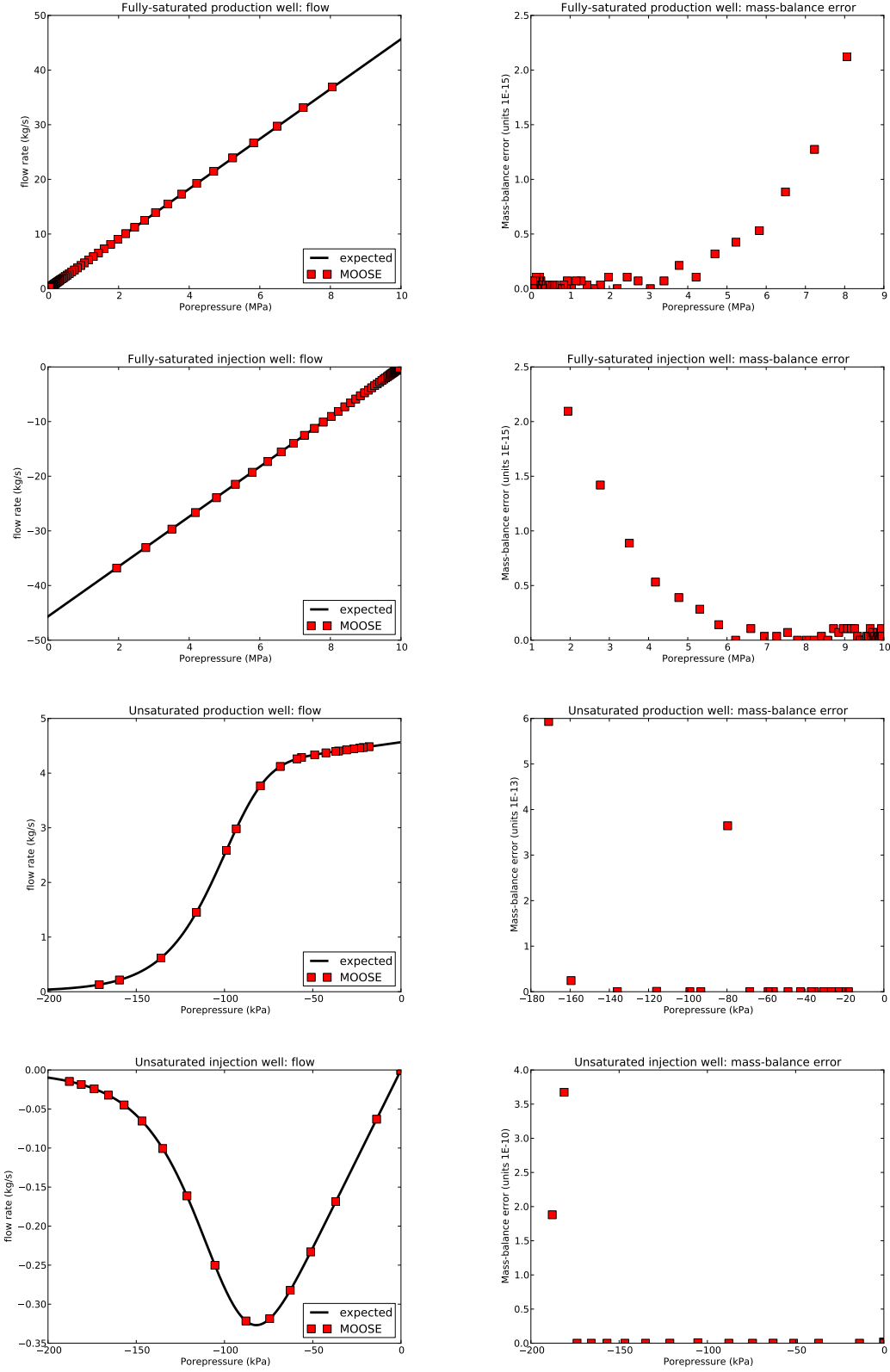
Figure 3.1: Left figures: Comparison between the MOOSE result (in dots), and the expected behaviour of the borehole flux given by Eqn (3.1) (as a line) for the cases listed in the text. Right figures: The mass balances, which are all small.
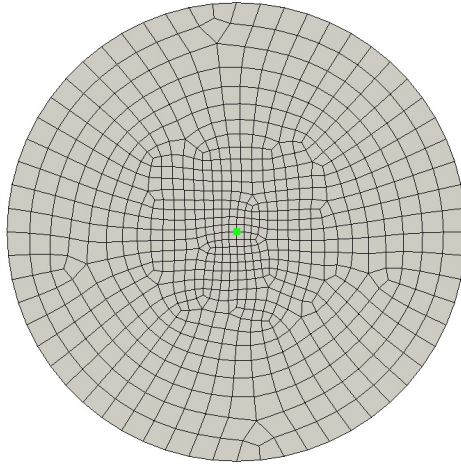
Figure 3.2: The mesh used in the comparison with Eqn (3.4), with the green dot indicating the position of the borehole. The central elements are $10 \times 10 \, \text{m}^2$, and the outer boundary is at $r = 300 \, \text{m}$.
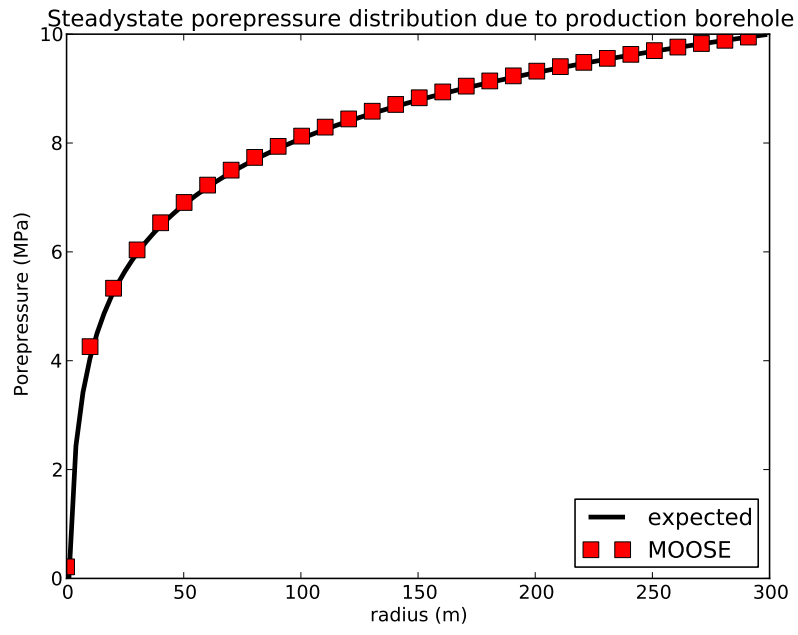
Figure 3.3: Comparison of the MOOSE results (dots) with the analytical solution Eqn (3.4) for the steadystate porepressure distribution surrounding single borehole.

Chapter 4

PorousFlow sink boundary conditions

A number of different sink boundary conditions have been implemented in PorousFlow. (To make these into sources instead of sinks, the strength of the flux just needs to be made negative.) All the sinks are implemented using full upwinding. This is to prevent the sink from attempting to remove fluid from a node that actually contains no fluid.

The basic sink uses a Function to specify the flux on the boundary, and also has the option of multiplying by any combination of: the fluid mobility, the relative permeability, or a mass fraction. These latter multiplying factors are all useful in the case of sinks to prevent an unlimited amount of fluid being withdrawn from the porous medium, which can lead to extremely poor nonlinear convergence even if only one node in the entire mesh is "running dry".

Derived from the basic one, is another boundary condition that allows the flux to be modified by a piecewise-linear function of porepressure, which is useful for the case where transfer coefficients are defined across the boundary, or more complicated situations.

Also derived from the basic one are two others, in which the flux is governed by a half Gaussian or half cubic function of porepressure, which are useful for modelling evapotranspiration through a boundary.

4.1 Basic sink

4.1.1 Test 1

A sink flux of strength $6 \, \mathrm{kg.m^{-2}.s^{-1}}$ is applied to the left edge ($x = 0$) of a 3D mesh. A single-phase, single-component fluid is used, and the porepressure is initialised to $p = y + 1$ (for $0 \le y \le 1$). No fluid flow within the element is used, so the masses of fluid at the finite-element nodes behave independently. The fluid is assumed to have density $\rho = 1.1 \exp(p/1.3) \, \mathrm{[kg.m^{-3}]}$. The porosity is 0.1.

Under these conditions, assuming $p \geq 0$ so that the porous medium is fully saturated with fluid, the fluid mass at a node should obey

$$m = V\phi\rho = V \times 0.1 \times 1.1 \exp(p/1.3) = m(t = 0) - 6At \;, \tag{4.1}$$

where V is the volume occupied by the node, and A is its area exposed to the flux. MOOSE correctly produces this result, as illustrated in Figure 4.1.
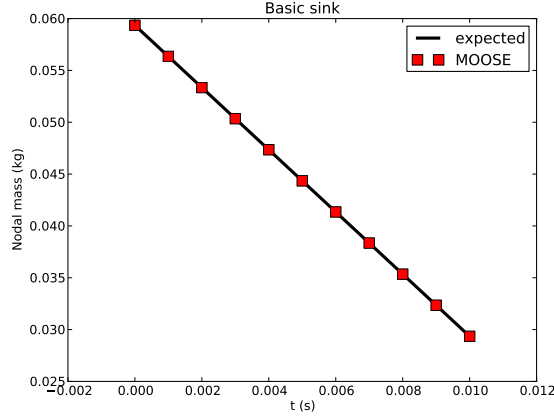

Figure 4.1: Results of Test 1, illustrating that MOOSE correctly applies a constant sink flux to boundary nodes.

4.1.2 Test 2

An identical setup to Test 1 is used here, but with the sink flux strength being multiplied by the mobility:

$$\text{mobility} = n_i k_{ij} n_j \rho / \nu \;, \tag{4.2}$$

where $n_i k_{ij} n_j$ is the permeability tensor k projected onto the normal direction to the boundary n, and the fluid density and viscosity are ρ and ν, respectively. In this example $\nu = 1.1\,\text{Pa.s}$ and $n_i k_{ij} n_j = 0.2\,\text{m}^2$. The other parameters are the same as Test 1, except now the strength of the flux is $6\,\text{Pa.s}^{-1}$.

In this case, the expected result is (for $p > 0$)

$$\frac{\mathrm{d}m}{\mathrm{d}t} = V\phi\frac{\mathrm{d}\rho}{\mathrm{d}t} = -6A\frac{n_i k_{ij} n_j \rho}{\mu} \;. \tag{4.3}$$

MOOSE correctly produces this result, as illustrated in Figure 4.2.
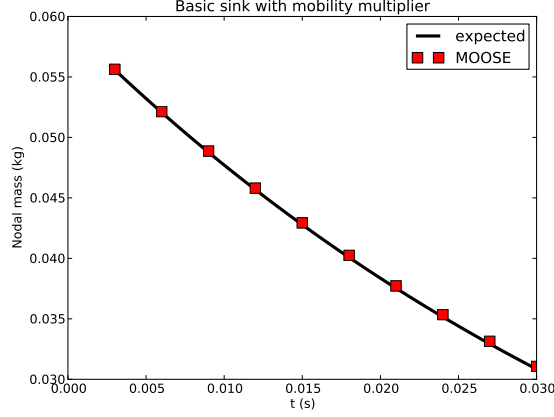
17

Figure 4.2: Results of Test 2, illustrating that MOOSE correctly applies a constant sink flux modified by the fluid mobility. (A slight drift away from the expected result is due to MOOSE taking large time steps.)

4.1.3 Test 3

An identical setup to Test 1 is used here, but with the sink flux strength being multiplied by the relative permeability, which is chosen to be:

$$\kappa_{\text{rel}} = S^2 \ , \tag{4.4}$$

with S being the fluid saturation. A van-Genuchten capillary relationship is used:

$$S = \left(1 + (-\alpha p)^{1/(1-m)}\right)^{-m} \ , \tag{4.5}$$

with $\alpha = 1.1 \, \text{Pa}^{-1}$, and $m = 0.5$. The porepressure is initialised to be $p = -y$. The other parameters are identical to Test 1.

In this case, the expected result is

$$\frac{\text{d}m}{\text{d}t} = V\phi\frac{\text{d}\rho S}{\text{d}t} = -6AS^2 \ . \tag{4.6}$$

MOOSE correctly produces this result, as illustrated in Figure 4.3.

4.1.4 Test 4

A similar setup to Test 1 is used here, but with a 3-component, single-phase fluid, with the sink flux only extracting the second component, with a rate proportional to the mass fraction of that component. This test checks that the flux is correctly implemented (see Figure 4.4) and that the correct fluid component is being withdrawn from the correct nodes. MOOSE produces the expected result.
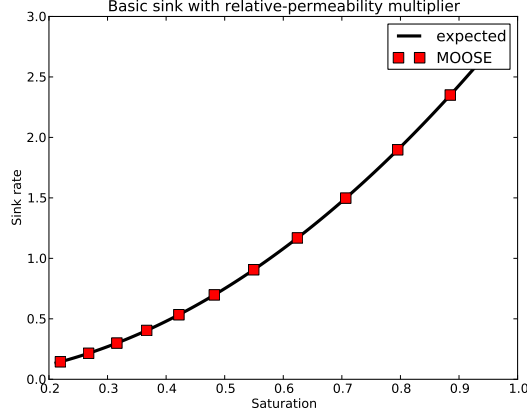
18

Figure 4.3: Results of Test 3, illustrating that MOOSE correctly applies a constant sink flux modified by the fluid relative permeability.
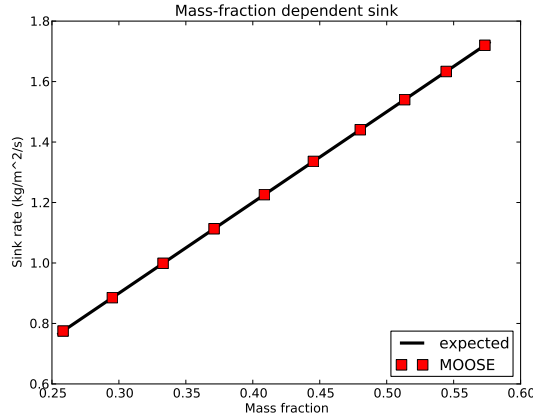

Figure 4.4: Results of Test 4, illustrating that MOOSE correctly applies a sink flux of a particular fluid component proportional to the component's mass fraction.

4.1.5 Test 5

A sink is applied to the left edge $(x = 0)$ of a 3D mesh. A 3-component, 2-phase fluid is used. Call the two phases "water" and "gas". The porepressures are initialised to $p_{\text{water}} = y$ and $p_{\text{gas}} = y + 3$. The mass fractions are initialised to $(0.3, 0.35, 0.35)$ in the water phase, and $(0.1, 0.8, 0.1)$ in the gas phase. The water phase is assumed to have density $\rho_{\text{water}} = 1.5 \exp(p_{\text{water}}/2.3)$, and the gas phase $\rho_{\text{gas}} = 1.1 \exp(p_{\text{gas}}/1.3)$. A van-Genuchten capillary relationship is used:

$$S_{\text{water}} = \left(1 + (\alpha(p_{\text{gas}} - p_{\text{water}})^{1/(1-m)}\right)^{-m} \ ,\qquad(4.7)$$

with $\alpha = 1.1\,\text{Pa}^{-1}$, and $m = 0.5$. The water relative permeaility is assumed to be Corey type with exponent 1, and the gas phase has exponent 2 (that is $\kappa_{\text{rel,gas}} = S^2_{\text{gas}}$, with $S_{\text{gas}} = 1 - S_{\text{water}}$).

The sink flux acts only on the second component. It is multiplied by the relative permeability

19

of the gas phase, and the mass fraction of the second component in the gas phase. This is possibly meaningless physically, but acts as a good test of the PorousFlowSink. In this test the mass fractions remain fixed: there is nothing to induce a change of a component from the water phase to the gas phase since the only Kernels used are mass-conservation Kernels that simply demand mass conservation of each fluid component (summed over each phase).

The test checks whether MOOSE is correctly applying the sink flux, and that the fluid-component masses at the nodes respond correctly to the flux. Figure 4.5 demonstrates that MOOSE produces the expected result.
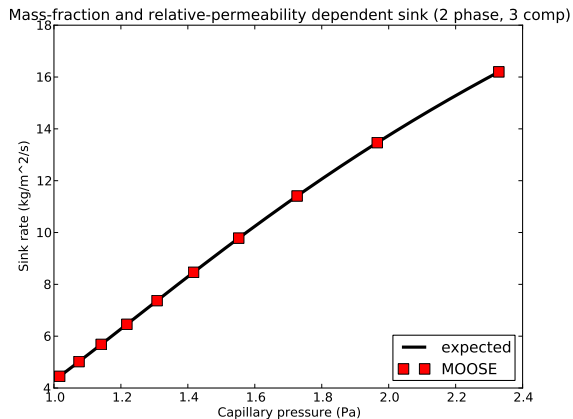

Figure 4.5: Results of Test 5, illustrating that in a 2-phase system MOOSE correctly applies a sink flux of a particular fluid component proportional to the component's mass fraction and the relative permeaility of the gas phase.

4.2 Piecewise-linear sink

A sink flux of strength

$$
f = \begin{cases} 8 & \text{if } p > 0.8 \\ 8(p + 0.2) & \text{if } 0.3 \le p \le 0.8 \\ 4 & \text{if } p < 0.3 \text{ ,} \end{cases} \tag{4.8}
$$

(measured in $\text{kg.m}^{-2}.\text{s}^{-1}$) is applied to the right side ($x = 1$) of a 3D mesh. A single-phase, single-component fluid is used, and the porepressure is initialised to $p = y + 1$ (for $0 \le y \le 1$). No fluid flow within the element is used, so the masses of fluid at the finite-element nodes behave independently. The fluid is assumed to have density $\rho = 1.1 \exp(p/1.3)$ $[\text{kg.m}^{-3}]$. The porosity is 0.1.

Under these conditions, the expected result for the fluid mass at a node on the right side of the mesh is

$$
\frac{\mathrm{d}m}{\mathrm{d}t} = V\phi \frac{\mathrm{d}\rho S}{\mathrm{d}t} = -fA \text{ .} \tag{4.9}
$$

The notation is the same as in previous sections.

The test checks that the mass evolves according to this equation, and that the flux is applied correctly. Figure 4.6 demonstrates agreement with the expected flux and the MOOSE implementation.

Figure 4.6: A piecewise-linear sink flux is correctly modelled by MOOSE

4.3   Half-Gaussian sink

A sink flux of strength

$$f = \begin{cases} 6 & \text{if } p \geq 0.9 \\ 6 \exp\left(-\frac{1}{2}\left(\frac{p-0.9}{0.5}\right)^2\right) & \text{if } p < 0.9 \ . \end{cases}$$

(4.10)

(measured in $\mathrm{kg.m^{-2}.s^{-1}}$) is applied to the right side ($x = 1$) of a 3D mesh. This is a half-Gaussian sink with center $0.9\,\mathrm{Pa}$, standard deviation $0.5\,\mathrm{Pa}$ and maximum 6. A single-phase, single-component fluid is used, and the porepressure is initialised to $p = y + 1.4$ (for $0 \leq y \leq 1$). No fluid flow within the element is used, so the masses of fluid at the finite-element nodes behave independently. The fluid is assumed to have density $\rho = 1.1 \exp(p/1.3)$ [$\mathrm{kg.m^{-3}}$]. The porosity is 0.1. A van-Genuchten capillary relationship is used:

$$S = \left(1 + (-\alpha p)^{1/(1-m)}\right)^{-m} \ ,$$

(4.11)

with $\alpha = 1.1\,\mathrm{Pa^{-1}}$, and $m = 0.5$.

Under these conditions, the expected result for the fluid mass at a node on the right side of the mesh is

$$\frac{\mathrm{d}m}{\mathrm{d}t} = V\phi\frac{\mathrm{d}\rho S}{\mathrm{d}t} = -fA \ .$$

(4.12)

The notation is the same as in previous sections.

The test checks that the mass evolves according to this equation, and that the flux is applied correctly. Figure 4.7 demonstrates agreement with the expected flux and the MOOSE implementation.
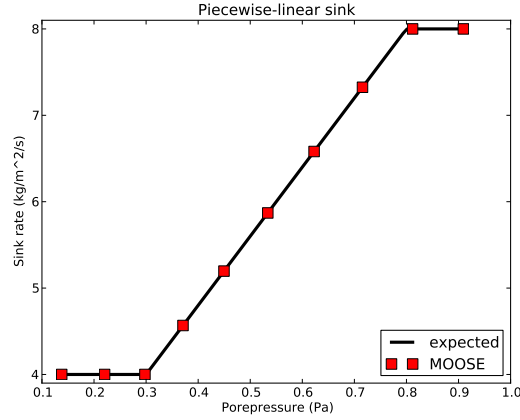
Figure 4.7: A half-Gaussian sink flux with center 0.9 Pa and standard deviation 0.5 Pa is correctly modelled by MOOSE

4.4 Half-cubic sink

A sink flux of strength

$$
f = \begin{cases} 3 & \text{if } p \geq 0.9 \\ \frac{3}{(-0.8)^3}(2(p - 0.9) + 0.8)(p - 0.9 + 0.8)^2 & \text{if } 0.1 < p < 0.9 \\ 0 & \text{if } p \leq 0.1 \end{cases}
\tag{4.13}
$$

(measured in $\text{kg.m}^{-2}.\text{s}^{-1}$) is applied to the right side ($x = 1$) of a 3D mesh. This is a half-cubic sink with center 0.9 Pa, cutoff -0.8 Pa, and maximum $3\,\text{kg.m}^{-2}.\text{s}^{-1}$. A single-phase, single-component fluid is used, and the porepressure is initialised to $p = x(y + 1)$ (for $0 \leq y \leq 1$ and $0 \leq x \leq 1$). No fluid flow within the element is used, so the masses of fluid at the finite-element nodes behave independently. The fluid is assumed to have density $\rho = 1.1 \exp(p/1.3)$ [kg.m^{-3}]. The porosity is 0.1.

Under these conditions, the expected result for the fluid mass at a node on the right side of the mesh is

$$
\frac{\mathrm{d}m}{\mathrm{d}t} = V\phi\frac{\mathrm{d}\rho S}{\mathrm{d}t} = -fA \ .
\tag{4.14}
$$

The notation is the same as in previous sections.

The test checks that the mass evolves according to this equation, and that the flux is applied correctly. Figure 4.8 demonstrates agreement with the expected flux and the MOOSE implementation.
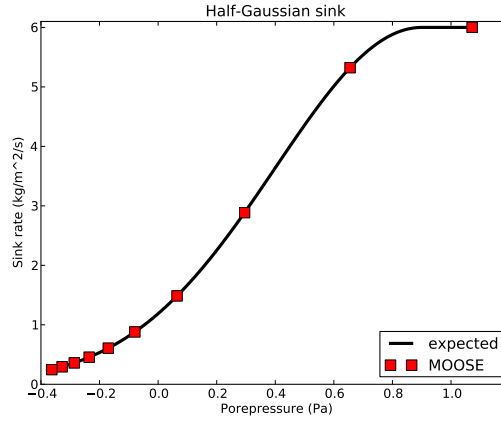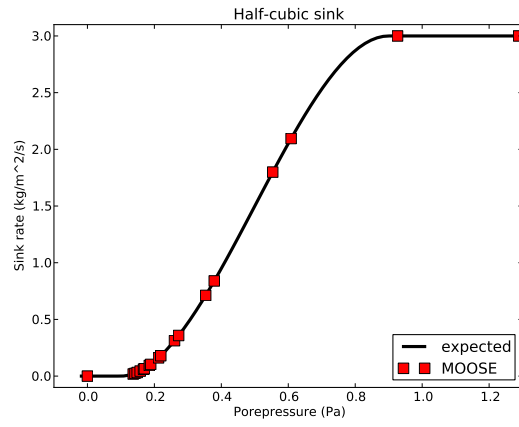
Figure 4.8: A half-cubic sink with center $0.9\,\mathrm{Pa}$, cutoff $-0.8\,\mathrm{Pa}$, and maximum $3\,\mathrm{kg.m^{-2}.s^{-1}}$ is correctly modelled by MOOSE.

Chapter 5

Advection of a fluid component

The porepressure at a boundary may be maintained at a fixed value by applying a sufficiently strong piecewise-linear sink:

$$f = Cp ,$$
(5.1)

(measured in kg.m^{-2}.s^{-1}) for large[1] conductance C. In the multi-component case, the flux of of fluid component κ should be made proportional to the component mass fraction, χ^κ:

$$f^\kappa = C\chi^\kappa p .$$
(5.2)

This is a "natural" boundary condition, in that fluid exits or enters the porous material at a rate dictated by the mass-fraction within the porous material. This means, for instance, that if fluid is exiting ($p > 0$ in this case) then only components that exist at the boundary system will exit, and MOOSE will not attempt to extract fluid components that have zero mass-fraction.

This example concerns a 1D porous material occupying the space $0 \leq x \leq 1$. It contains a single phase fluid with two fluid components. The porous material initially only contains fluid component 1, and there is a pressure gradient:

$$p(t = 0) = 1 - x \quad \text{and} \quad \chi^0(t = 0) = 0 .$$
(5.3)

For $t > 0$, fluid component 0 is introduced on the material's left side ($x = 0$), by applying the fixed boundary conditions:

$$p(x = 0) = 1 \quad \text{and} \quad \chi^0(x = 0) = 1 .$$
(5.4)

The right-hand side, at $x = 1$, is subjected to the flux of Eqn (5.2). The fluid-component 0 flows from the left side to the right side via the pressure gradient. To simplify the following analysis, the fluid bulk modulus is taken to be very large.

Because the fluid bulk modulus is very large, $\partial P/\partial x = -1$ is a solution for all time. This means that the governing equation reduces to

$$\phi \frac{\partial \chi}{\partial t} = (k_{ij}/\mu)\nabla_j \chi \nabla_i P .$$
(5.5)

---

[1]If C is too large then it will dominate the numerics and MOOSE will not converge.

In this equation ϕ is the porosity, k_{ij} is the permeability tensor, and μ is the fluid viscosity. This is just the advection equation for the mass fraction χ, with velocity

$$\text{velocity}_j = \nabla_i P \frac{k_{ij}}{\mu\phi} \ .$$

(5.6)

In this test, the parameters are chosen such that velocity$= 1\,\text{m.s}^{-1}$.

The sharp front (described by the advection equation with the initial and boundary conditions) is *not* maintained by MOOSE. This is due to numerical diffusion, which is particularly strong in the upwinding scheme implemented in the PorousFlow module. Nevertheless, MOOSE advects the smooth front with the correct velocity, as shown in Figure 5.1.

The sharp front is *not* maintained by MOOSE even when no upwinding is used. In the case at hand, which uses a fully-saturated single-phase fluid, the `FullySaturated` versions of the Kernels may be used in order to compare with the standard fully-upwinded Kernels. The `FullySaturated` Kernels do not employ any upwinding whatsoever, so less numerical diffusion is expected. This is demonstrated in Figure 5.1. Two additional points may also be nocied: (1) the lack of upwinding has produced a "bump" in the mass-fraction profile near the concentrated side; (2) the lack of upwinding means the temperature profile moves slightly slower than it should. These two affects reduce as the mesh density is increased, however.
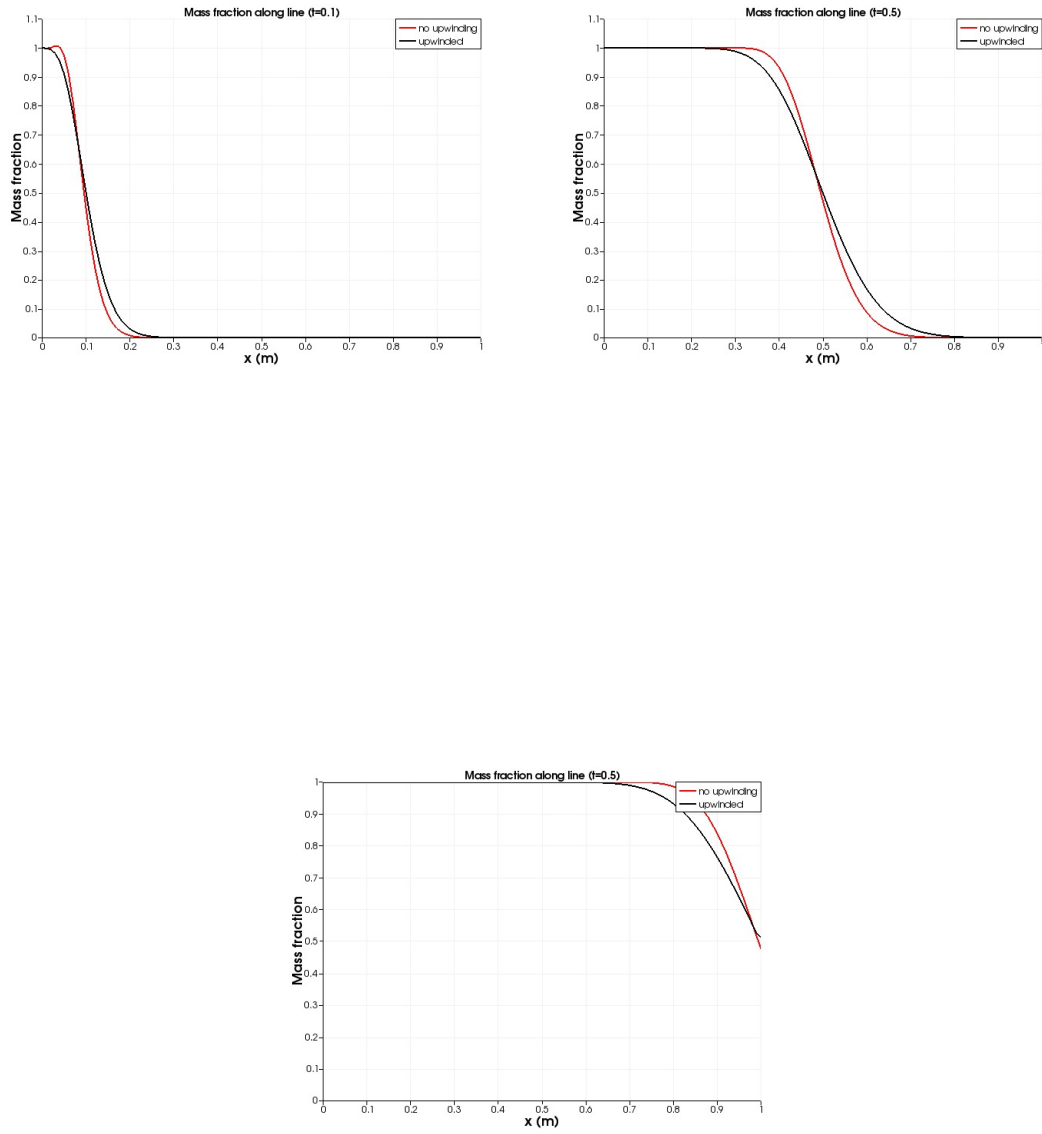
Figure 5.1: Results of the advection of a fluid component test, illustrating that the numerical implementation of porous flow within MOOSE diffuses sharp fronts, but advects them at the correct velocity ($v = 1\,\mathrm{m.s^{-1}}$ in this case, and notice the centre of the front is at the correct position in each picture). Less diffusion is experienced when upwinding is not used. Top left: mass fraction at $t = 0.1\,\mathrm{s}$. Top right: mass fraction at $t = 0.5\,\mathrm{s}$. Bottom: mass fraction at $t = 1.0\,\mathrm{s}$.

Chapter 6

Gravity equilibrium

6.1 Establishment of gravity head in 1D

These tests concern the steadystate pressure distribution obtained either by running a transient model for a long time, or by running a steady-state analysis, both of which should lead to the same result. Without fluxes, the steadystate pressure distribution is just

$$P(x) = P_0 - \rho_0 g x \ , \tag{6.1}$$

if the fluid bulk modulus, B, is large enough compared with P. Here P_0 is the porepressure at $x = 0$. For smaller bulk modulus

$$P(x) = -B \log \left(e^{-P_0/B} + \frac{g \rho_0 x}{B} \right) \ . \tag{6.2}$$

Here it is assumed that the density is given by $\rho = \rho_0 e^{-P/B}$ with constant bulk modulus, g is the magnitude acceleration due to gravity (a vector assumed to be pointing in the negative x direction), and x is position. The tests described below are simple tests and are part of the automatic test suite.

6.2 Single-phase, single-component

Two single-phase simulations with 100 1D elements are run: one with fully-saturated conditions, and the other with unsaturated conditions using the van-Genuchten capillary pressure (this should not, and does not, make any difference to the results). The porepressure is held fixed at one boundary ($x = 0$).

An example verification is shown in Figure 6.1, which also shows results from a 2-phase simulation (see Section 6.3).
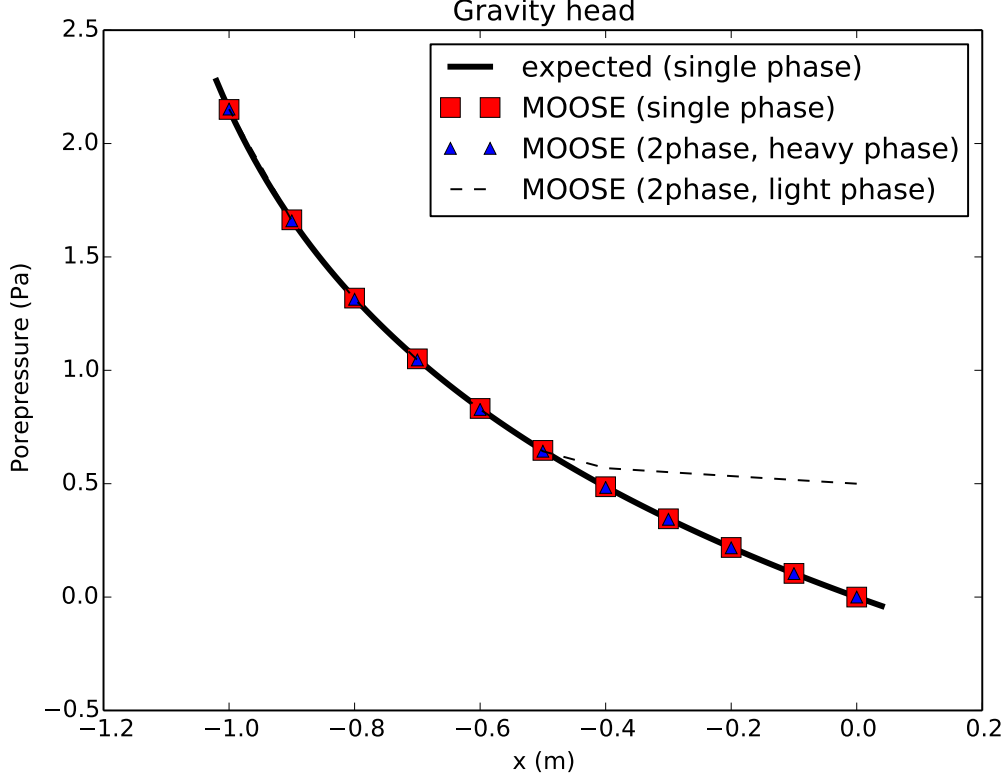
Figure 6.1: Comparison between the MOOSE result (in dots), and the exact analytic expression given by Eqn (6.2). test had 10 elements in the x direction, with $-1 \leq x \leq 0$ m. The parameters were $B = 1.2$ Pa, $\rho_0 = 1$ kg.m^{-3}, and $g = -1$ m.s^{-2}. For the two-phase simulation, the light phase had $B = 1$ Pa and $\rho_0 = 0.1$ kg.m^{-2}.

6.3 Two-phase, two-component

Two-phase, two-component simulations may also be checked against Eqn (6.2). Four simulations are performed.

One steady-state simulation is performed. Steady-state simulations are more difficult to perform in two-phase situations because of the inherently stronger nonlinearities, but mostly because simulations can easily enter unphysical domains (negative saturation, for instance) without the stabilising presence of the mass time-derivative.

Three transient simulations are performed. In the transient simulations, conservation of mass can be checked, and the tests demonstrate MOOSE conserves mass. Depending on the initial and boundary conditions, the "heavy" phase (with greatest mass) can completely displace the "light" phase, which is forced to move to the top of the simulation. In this case Eqn (6.2) only governs the light phase in the unsaturated zone, since in the saturated zone (where there is zero light phase) the pressure must follow the heavy-phase version of Eqn (6.2). An example is shown in Figure 6.1.

Chapter 7

Presssure-pulse in 1D

Richards' equation for flow through a fully saturated medium without gravity and without sources is just Darcy's equation

$$\frac{\partial}{\partial t}\phi\rho = \nabla_i\left(\frac{\rho\kappa_{ij}}{\mu}\nabla_j P\right) \ , \tag{7.1}$$

with notation described in the Theory Manual. Using $\rho \propto \exp(P/K)$, where K is the fluid bulk modulus, Darcy's equation becomes

$$\frac{\partial}{\partial t}\rho = \nabla_i\alpha_{ij}\nabla\rho \ , \tag{7.2}$$

with

$$\alpha_{ij} = \frac{\kappa_{ij}B}{\mu\phi} \ . \tag{7.3}$$

Here I've assumed the porosity and bulk modulus are constant in space and time.

Consider the one-dimensional case were the spatial dimension is the semi-infinite line $x \geq 0$. Suppose that initially the pressure is constant, so that

$$\rho(x, t = 0) = \rho_0 \quad \text{for} \quad x \geq 0 \ . \tag{7.4}$$

Then apply a fixed-pressure Dirichlet boundary condition at $x = 0$ so that

$$\rho(x = 0, t > 0) = \rho_\infty \tag{7.5}$$

The solution of the above differential equation is well known to be

$$\rho(x, t) = \rho_\infty + (\rho_0 - \rho_\infty)\,\mathrm{Erf}\left(\frac{x}{\sqrt{4\alpha t}}\right) \ , \tag{7.6}$$

where Erf is the error function.

This is verified by using the following tests on a line of 10 elements.

1. Steady state 1-phase analysis to demonstrate that the steady-state of $\rho = \rho_\infty$ is achieved.

2. Transient 1-phase analysis.

3. Transient 1-phase, 3 component analysis to check that the components diffuse at the same rate.

4. Transient 2-phase analysis, with the "water" state fully saturated.

An example verification is shown in Figure 7.1. These are part of the automatic test suite.
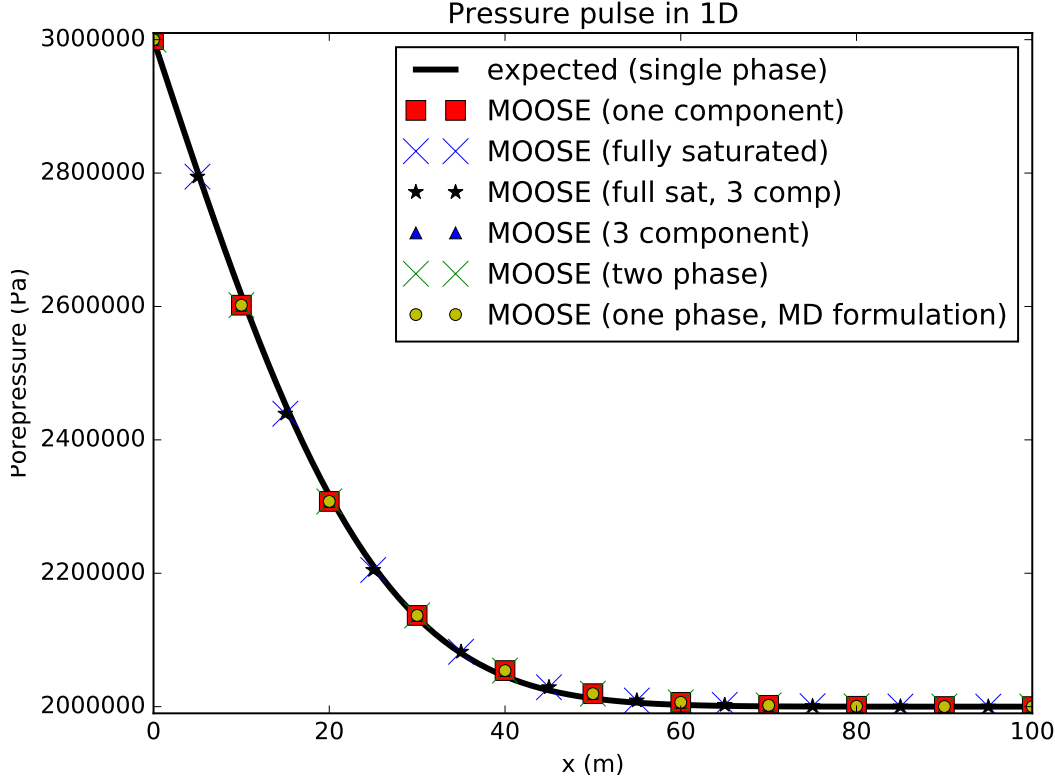
Figure 7.1: Comparison between the MOOSE result (in dots), and the exact analytic expression given by Eqn (12.10). This test had 10 elements in the x direction, with $0 \leq x \leq 100\,\mathrm{m}$, and ran for a total of 10^4 seconds with 10 timesteps. The parameters were $B = 2\,\mathrm{GPa}$, $\kappa_{xx} = 10^{-15}\,\mathrm{m}^2$, $\mu = 10^{-3}\,\mathrm{Pa.s}$, $\phi = 0.1$, with initial pressure $P = 2\,\mathrm{MPa}$, and applied pressure $P = 3\,\mathrm{MPa}$ at $x = 0$. For greater spatial resolution and smaller timesteps the agreement increases. Both the multi-component single-phase simulation (using the fully-saturated non-upwinding Kernels and the partially-saturated full-upwinding Kernels) and the 2-phase fully-water-saturated simulation give identical results for the water porepressure.

Chapter 8

Diffusion and dispersion

8.1 Diffusion

The results of MOOSE are compared with the classical diffusion profile for a simple 1D model with mass diffusion. In this example, the left end of the mesh is held at a constant mass fraction of 1, while the right hand end is prescribed a zero mass fraction boundary condition. No advection takes place, so mass transfer is by diffusion only. This concentration profile has a well-known similarity solution given by

$$C(u) = \text{erfc}(u), \tag{8.1}$$

where $\text{erfc}(u)$ is the complentary error function, and $u = x/(2\sqrt{Dt})$ is the similarity solution, x is distance, t is time, and D is the diffusion coefficient.

The comparison between MOOSE and the analytical solution is presented in Figure **??**, where we observe a very good agreement between the two solutions.

8.2 Hydrodynamic dispersion

The MOOSE results are compared to known analytical solutions for simple problems in order to vertify that the MOOSE implementation is working properly. For a simple 1D model with no diffusion and constant velocity v, an analytical solution for the mass fraction profile is given
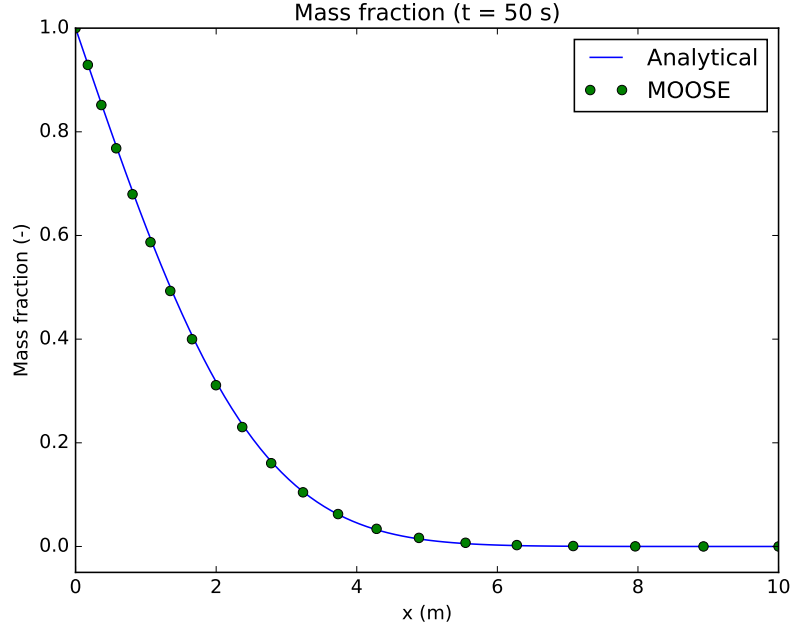
Figure 8.1: Mass fraction profile from diffusion only

by Javendel et al. (1984)[1],

$$
\begin{aligned}
C(x, t) = C_0 & \left\{ \frac{1}{2} \operatorname{erfc}\left(\frac{x - vt}{2\sqrt{Dt}}\right) + \left(\frac{v^2 t}{\pi D}\right)^{1/2} \exp\left(-\frac{[x - vt]^2}{4DT}\right) \right. \\
& \left. - \frac{1}{2}\left(1 + \frac{vx}{D} + \frac{v^2 t}{D}\right) \exp\left(\frac{vx}{D}\right) \operatorname{erfc}\left(\frac{x + vt}{2\sqrt{DT}}\right) \right\},
\end{aligned}
\tag{8.2}
$$

where all parameters have been previously defined.

The comparison between the automatic test problem *disp01* and the analytical solution is presented in Figure 8.2. The MOOSE results do not coincide with the analytical solution near the top and bottom of the concentration front due to numerical dispersion. If the number of elements in the mesh is increased and the time step size is reduced, numerical dispersion is reduced and a much closer fit to the analytical solution is obtained, see Figure 8.3. This second test is marked as heavy as it takes approximately 5 seconds to run, but is available in the automatic test suite.

---

[1]Javandel, I, Doughty, C, Tsang, C-f, Groundwater Transport, Handbook of Mathematical Models, AGU, 1984
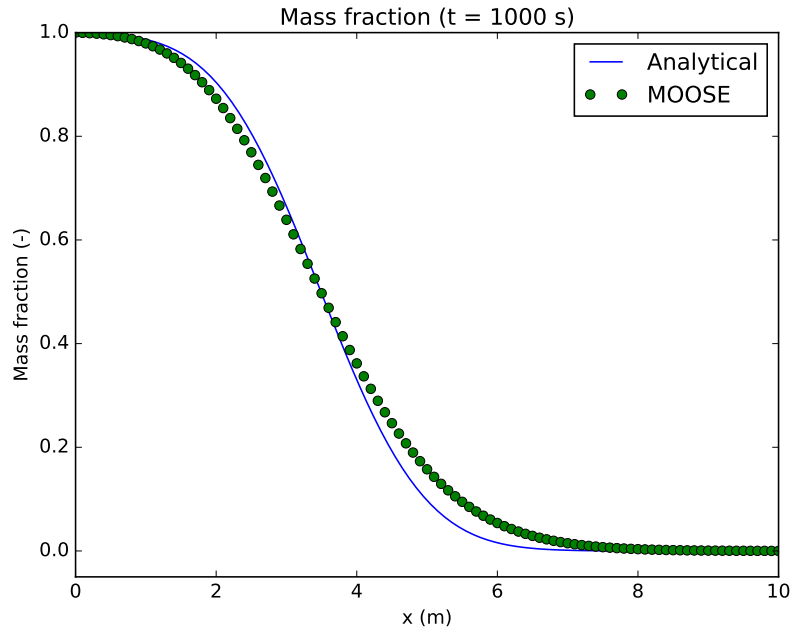
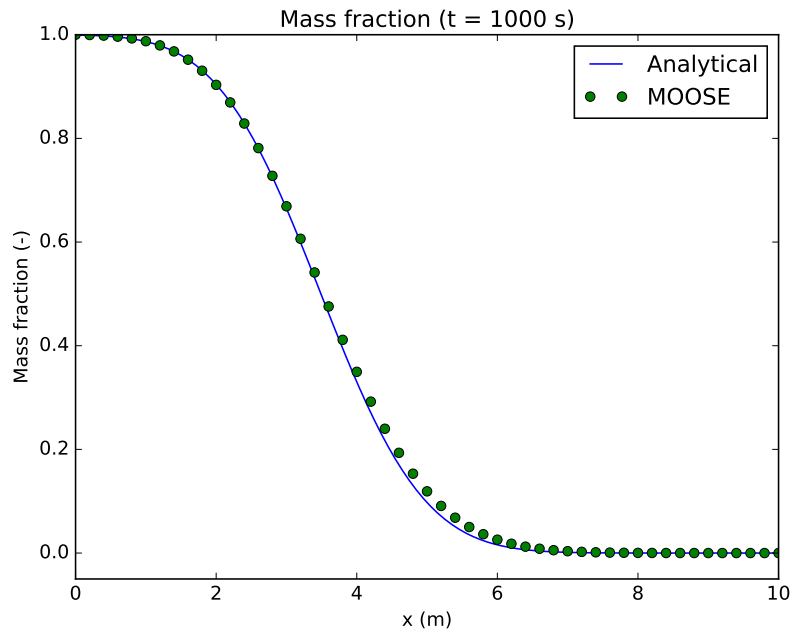Figure 8.2: Mass fraction profile from hydrodynamic dispersion only

Figure 8.3: Mass fraction profile from hydrodynamic dispersion only using a more refined grid and smaller time steps

Chapter 9

Infiltration problem

9.1 The 2-phase analytic infiltration solution

The physical setup studied in this section is a 1D column that is initially unsaturated, and which is subject to a constant injection of fluid from its top. This is of physical importance because it is a model of constant rainfall recharge to an initially dry groundwater system. The top surface becomes saturated, and this saturated zone moves downwards into the column, diffusing as it goes. The problem is of computational interest because under certain conditions an analytic solution is available for the saturation profile as a function of depth and time.

The Richards' equation for an incompressible fluid in one spatial dimension (z) reads

$$\dot{S} = \nabla \left(D \nabla S \right) - \nabla K \ , \tag{9.1}$$

where

$$D(S) \;=\; -\frac{\kappa \kappa_{rel}}{\mu \phi} P_{\mathrm{c}}' \ , \tag{9.2}$$

$$K(S) \;=\; \frac{\rho g \kappa \kappa_{\mathrm{rel}}}{\mu \phi} \ . \tag{9.3}$$

Here $P_{\mathrm{c}} = -P$ which is the capillary pressure, and recall that $P_{\mathrm{c}}'(S) < 0$.

The analytic solution of this nonlinear diffusion-advection relevant to constant infiltration to groundwater has been derived Broadbridge and White[1] for certain functions D and K. Broadbridge and White assume the hydraulic conductivity is

$$K(S) = K_n + (K_s - K_n)\frac{\Theta^2(C - 1)}{C - \Theta} \ , \tag{9.4}$$

where

$$\Theta = \frac{S - S_n}{S_s - S_s} \ , \tag{9.5}$$

---

[1]P Broadbridge, I White "Constant rate rainfall infiltration: A versatile nonlinear model, 1 Analytical solution". Water Resources Research 24 (1988) 145–154.

and the parameters obey $0 \leq K_n < K_s$, $0 \leq S_n \leq S \leq S_s \leq 1$, and $C > 1$. The diffusivity is of the form $a(b - S)^{-2}$. This leads to very complicated relationships between the capillary pressure, P_c, and the saturation, except in the case where K_n is small, when they are related through

$$\frac{P_c}{\lambda_s} = \frac{\Theta - 1}{\Theta} - \frac{1}{C} \log \left(\frac{C - \Theta}{(C - 1)\Theta} \right) , \tag{9.6}$$

with $\lambda_s > 0$ being the final parameter introduced by Broadbridge and White.

Broadbridge and White derive time-dependent solutions for constant recharge to one end of a semi-infinite line. Their solutions are quite lengthy, so I will not write them here. To compare with MOOSE, I use the following parameters — the hydraulic parameters are those used in Figure 3 of Broadbridge and White:

Bar length	$20\,\mathrm{m}$
Bar porosity	0.25
Bar permeability	1
Gravity	$0.1\,\mathrm{m.s}^{-2}$
Fluid density	$10\,\mathrm{kg.m}^{-3}$
Fluid viscosity	$4\,\mathrm{Pa.s}$
S_n	$0\,\mathrm{m.s}^{-1}$
S_s	$1\,\mathrm{m.s}^{-1}$
K_n	$0\,\mathrm{m.s}^{-1}$
K_s	$1\,\mathrm{m.s}^{-1}$
C	1.5
λ_s	$2\,\mathrm{Pa}$
Recharge rate R_*	0.5

Broadbridge and white consider the case where the initial condition is $S = S_s$, but this yields $P = -\infty$, which is impossible to use in a MOOSE model. Therefore the initial condition $P = -900\,\mathrm{Pa}$ is used which avoids any underflow problems. The recharge rate of $R_* = 0.5$ corresponds in the MOOSE model to a recharge rate of $0.5\rho\phi(\kappa_s - \kappa_n) = 1.25\,\mathrm{kg.m}^{-2}.\mathrm{s}^{-1}$. Note that I've chosen $\frac{\rho g \kappa}{\mu \phi} = 1\,\mathrm{m.s}^{-1}$, so that the K_n and K_s may be encoded as $\kappa_n = 0$ and $\kappa_s = 1$ in the relative permeability function Eqn (9.4) in a straightforward way.

Figure 9.1 shows good agreement between the analytic solution of Broadbridge and White and the MOOSE implementation. There are minor discrepancies for small values of saturation: these get smaller as the temporal and spatial resolution is increased, but never totally disappear due to the initial condition of $P = -900\,\mathrm{Pa}$.

Two tests are part of the automatic test suite (one is marked "heavy" because it is a high-resolution version).

9.2 The two-phase analytic drainage solution

Warrick, Lomen and Islas[2] extended the analysis of Broadbridge and White (Chapter 9.1) to include the case of drainage from a medium.

The setup is an initially-saturated infinitely-long column of material that drains freely from its lower end. This is simulated by placing a boundary condition of $P = 0$ at the lower end. To obtain their analytical solutions, Warrick, Lomen and Islas make the same assumptions as Broadbridge and White concerning the diffusivity and conductivity of the medium. Their solutions are quite lengthy, so I will not write them here.

A MOOSE model with the parameters almost identical to those listed in Chapter 9.1 is compared with the analytical solutions. The only differences are that the "bar" length is $10000\,\mathrm{m}$ (to avoid any interference from the lower Dirichlet boundary condition), and $R_* = 0$ since there is no recharge. The initial condition is $P = 10^{-4}\,\mathrm{Pa}$: the choice $P = 0$ leads to poor convergence since by construction the Broadbridge-White capillary function is only designed to simulate the unsaturated zone $P < 0$ and a sensible extension to $P \geq 0$ is discontinuous at $P = 0$.

Figure 9.2 shows good agreement between the analytic solution and the MOOSE implementation. Any minor discrepancies get smaller as the temporal and spatial resolution increase.

This test is part of the automatic test suite that is run every time the code is updated.

---

[2]AW Warrick, DO Lomen and A Islas, "An analytical solution to Richards' Equation for a Draining Soil Profile", Water Resources Research 26 (1990) 253–258.

bw.pdf

Figure 9.1: Comparison of the Broadbridge and White analytical solution with the MOOSE solution for 3 times. This figure is shown in the standard format used in the Broadbridge-White paper: the constant recharge is applied to the depth = 0 surface, and gravity acts downwards in this figure.
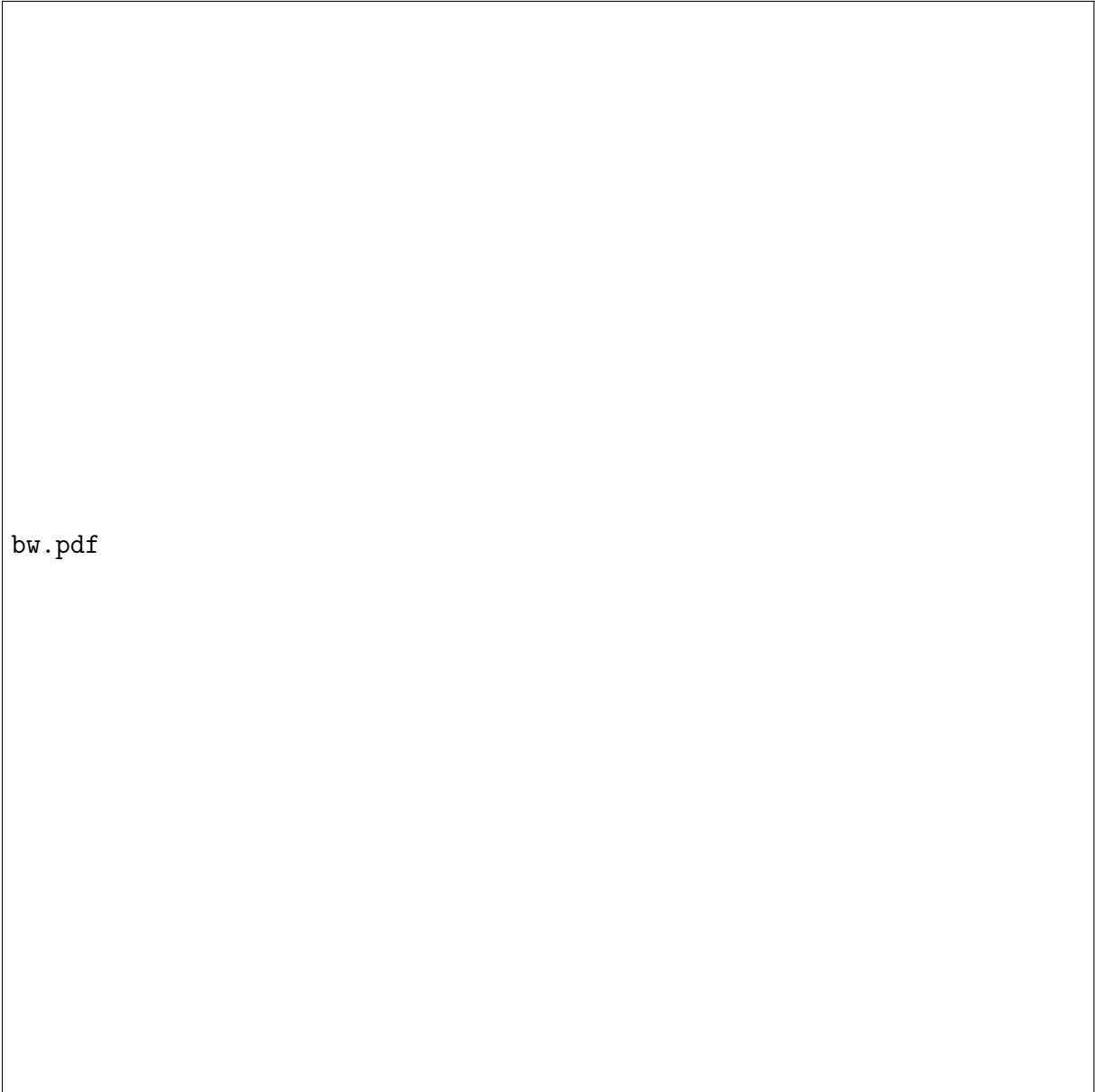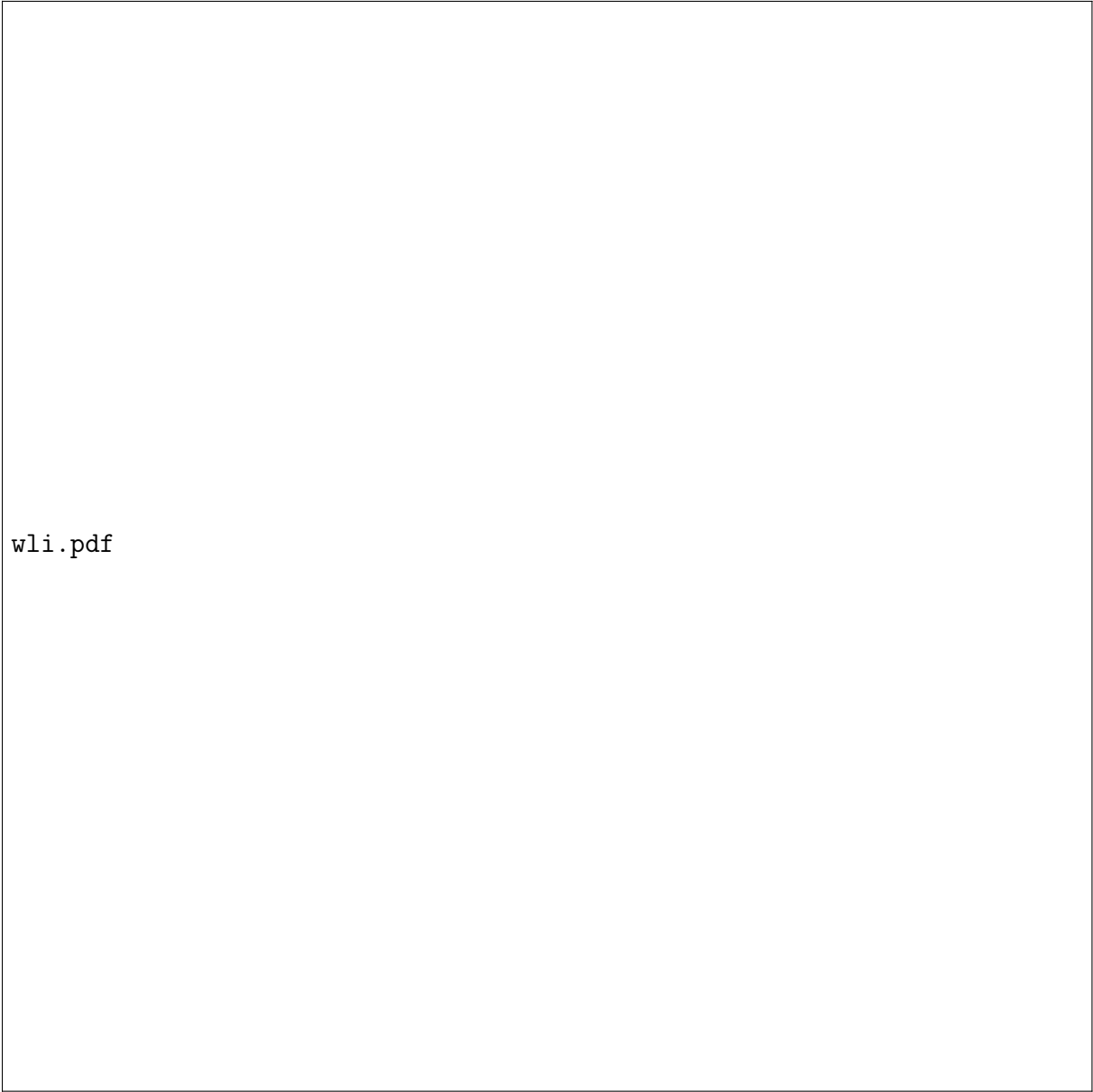
wli.pdf

Figure 9.2: Comparison of the Warrick, Lomen and Islas analytical solution with the MOOSE solution for 3 times. This figure is shown in the standard format used in the literature: the top of the model is depth = 0 surface, and gravity acts downwards in this figure, with fluid draining from depth = ∞.

Chapter 10

Single-phase infiltration and drainage

Forsyth, Wu and Pruess[1] describe a HYDRUS simulation of an experiment involving infiltration (experiment 1) and subsequent drainage (experiment 2) in a large caisson. The simulation is effectively one dimensional, and is shown in Figure 10.1.

The properties common to each experiment are:

Caisson	0.33
Caisson permeability	$2.95 \times 10^{-13}\,\mathrm{m}^2$
Gravity	$10\,\mathrm{m.s}^{-2}$
Water density	$1000\,\mathrm{kg.m}^{-3}$
Water viscosity	$0.00101\,\mathrm{Pa.s}$
Water bulk modulus	$20\,\mathrm{MPa}$
Water residual saturation	0.0
Air residual saturation	0.0
Air pressure	0.0
van Genuchten α	$1.43 \times 10^{-4}\,\mathrm{Pa}^{-1}$
van Genuchten m	0.336
van Genuchten turnover	0.99

In each experiment 120 finite elements were used along the length of the Caisson. The modified van-Genuchten relative permeability curve with a "turnover" (set at $S = 0.99$) was employed in order to improve convergence significantly. Hydrus also uses a modified van-Genuchten curve, although I couldn't find any details on the modification.

In experiment 1, the caisson is initially at saturation 0.303 ($P = -72620.4\,\mathrm{Pa}$), and water is pumped into the top with a rate $0.002315\,\mathrm{kg.m}^{-2}.\mathrm{s}^{-1}$. This causes a front of water to advance down the caisson. Figure 10.2 shows the agreement between MOOSE and the published result (this result was obtained by extracting data by hand from online graphics).

---

[1]PA Forsyth, YS Wu and K Pruess, "Robust numerical methods for saturated-unsaturated flow with dry initial conditions in heterogeneous media", Advances in Water Resources 18 (1995) 25–38

Figure 10.1: Two experimental setups from Forsyth, Wu and Pruess. Experiment 1 involves infiltration of water into an initially unsaturated caisson. Experiment 2 involves drainage of water from an initially saturated caisson.

In experiment 2, the caisson is initially fully saturated at $P = 0$, and the bottom is held at $P = 0$ to cause water to drain via the action of gravity. Figure 10.2 shows the agreement between MOOSE and the published result.

Experiment 1 and the first 4 simulation days of experiment 2 are marked as "heavy" in the PorousFlow test suite since the simulations take around 3 seconds to complete. This means they are not run by default every time the code is updated, and must be run manually. However, the final 96 days of experiment 2 run quickly and are part of the automatic test suite.
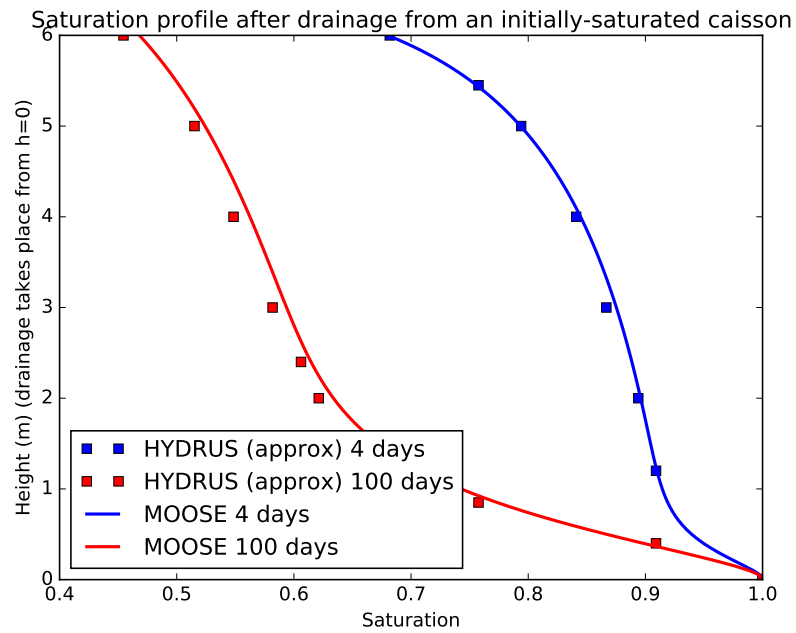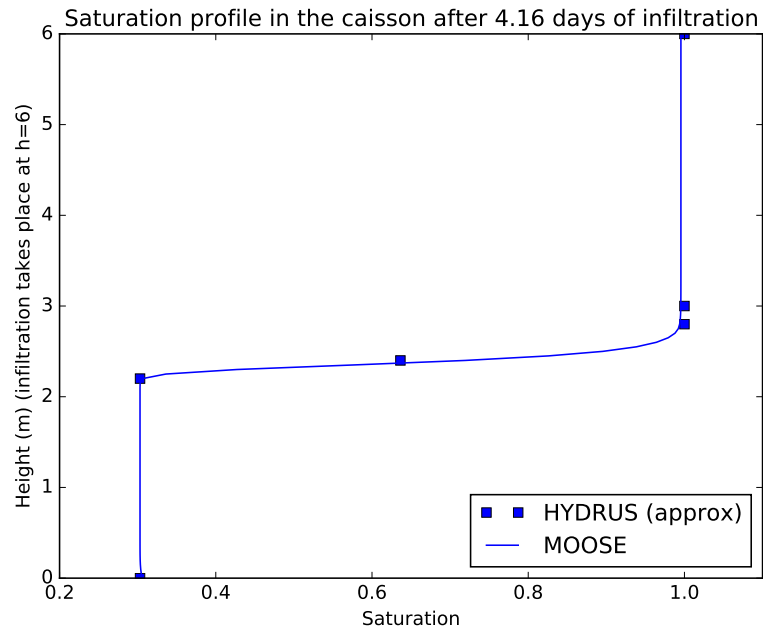
Figure 10.2: Saturation profiles in the caisson. Top: After 4.16 days of infiltration. Bottom: After drainage from an initially-saturated simulation (4 days and 100 days profiles). Note that the HYDRUS results are only approximate as I extrated the data by hand from online graphics.

Chapter 11

Water infiltration into a two-phase system

An analytic solution of the two-phase Richards' equations with gravity[1] on a semi-infinite line $z \geq 0$, with a constant water infiltration flux at $z = 0$ has been derived by Rogers, Stallybrass and Clements[2]. The authors assume incompressible fluids; linear relative permeability relationships; the "oil" (or "gas") viscosity is larger than the water viscosity; and, a certain functional form for the capillary pressure. When the oil viscosity is exactly twice the water viscosity, their effective saturation reads

$$S_{\mathrm{eff}} = \frac{1}{\sqrt{1 + \exp((P_c - A)/B)}} \ , \tag{11.1}$$

where $P_c = P_{\mathrm{oil}} - P_{\mathrm{water}}$ is the capillary pressure, and A and B are arbitrary parameters to be defined by the user in the MOOSE implementation. For other oil/water viscosity ratios $P_c = P_c(S_{\mathrm{eff}})$ is more complicated, and note that their formulation allows $P_c < 0$, but only the particular form Eqn (11.1) need be used to validate the MOOSE implementation.

RSC's solutions are quite lengthy, so I will not write them here. To compare with MOOSE, the following parameters are used:

---

[1]Unfortunately there must be a typo in the RSC paper as for nonzero gravity their results are clearly incorrect.

[2]C Rogers, MP Stallybrass and DL Clements "On two phase filtration under gravity and with boundary infiltration: application of a Backlund transformation" Nonlinear Analysis, Theory, Methods and Applications 7 (1983) 785–799

Bar length	$10\,\mathrm{m}$
Bar porosity	0.25
Bar permeability	$10^{-5}\,\mathrm{m}^2$
Gravity	$0\,\mathrm{m.s}^{-2}$
Water density	$10\,\mathrm{kg.m}^{-3}$
Water viscosity	$10^{-3}\,\mathrm{Pa.s}$
Oil density	$20\,\mathrm{kg.m}^{-3}$
Oil viscosity	$2 \times 10^{-3}\,\mathrm{Pa.s}$
Capillary A	$10\,\mathrm{Pa}$
Capillary B	$1\,\mathrm{Pa}$
Initial water pressure	$0\,\mathrm{Pa}$
Initial oil pressure	$15\,\mathrm{Pa}$
Initial water saturation	0.08181
Initial oil saturation	0.91819
Water injection rate	$1\,\mathrm{kg\,s}^{-1}\,\mathrm{m}^{-2}$

In the RSC theory water is injected into a semi-infinite domain, whereas of course the MOOSE implementation has finite extent ($0 \leq z \leq 10$ is chosen). Because of the near incompressibility of the fluids (I choose the bulk modulus to be $2\,\mathrm{GPa}$) this causes the porepressures to rise enormously, and the problem can suffer from precision-loss problems. Therefore, the porepressures are fixed at $z = 10$. This does not affect the progress of the water saturation front. Figure 11.1 shows good agreement between the analytic solution and the MOOSE implementation. Any minor discrepancies get smaller as the temporal and spatial resolution increase, as is suggested by the two comparisons in that figure.

The "low-resolution" test has 200 elements in $0 \leq z \leq 10$ and uses 15 time steps is part the automatic test suite that is run every time the code is updated. The "high-resolution" test has 600 elements and uses 190 time steps, and is marked as "heavy".

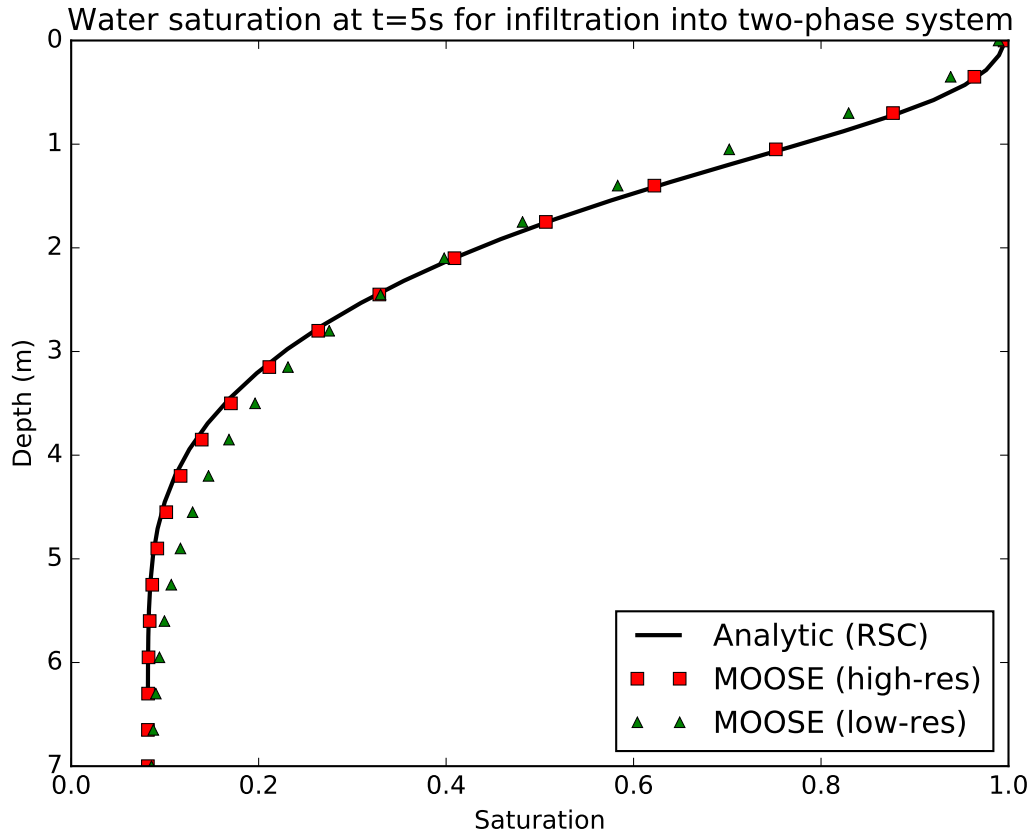Figure 11.1: Water saturation profile for $t = 5\,\mathrm{s}$ in the Rogers-Stallybrass-Clements test. The initial water saturation is 0.08181, and water is injected at the top of this figure at a constant rate. This forms a water front which displaces the oil. Black line: RSC's analytic solution. Red squares: high-resolution MOOSE simulation. Green triangles: lower resolution MOOSE simulation.

Chapter 12

Heat conduction

12.1 Simple heat conduction in 1D

Porous-flow heat conduction is governed by the equation

$$0 = \frac{\partial}{\partial t}\mathcal{E} + \nabla \cdot \mathbf{F}^{\mathrm{T}} \ , \tag{12.1}$$

Here $\mathcal{E}$ is the energy per unit volume in the rock-fluid system, and $\mathbf{F}^{\mathrm{T}}$ is the heat flux. In the porous-flow module

$$\mathcal{E} = (1 - \phi)\rho_R C_R T + \phi \sum_{\mathrm{ph}} S_{\mathrm{ph}}\rho_{\mathrm{ph}}\mathcal{E}_{\mathrm{ph}} \ , \tag{12.2}$$

when there is no adsorbed species. Here T is the temperature, ϕ is the rock porosity, and S_{ph} is the saturation of phase ph. The remainder of the notation is described in the next paragraph. When studying problems involving heat conduction (with no fluid convection)

$$\mathbf{F}^{\mathrm{T}} = -\lambda\nabla T \ , \tag{12.3}$$

where λ is the tensorial thermal conductivity of the rock-fluid system.

The tests described in this section use the following simple forms for each term

- ρ_R, which is the rock-grain density (that is, the density of rock with zero porespace), measured in kg.m^{-3}, is assumed constant in the current implementation of the PorousFlow module.

- C_R, which is the rock-grain specific heat capacity, measured in J.kg^{-1}.K^{-1}, is assumed constant in the current implementation of the PorousFlow module.

- ρ_{ph}, which is the density of fluid phase ph, is assumed in this chapter to be a function of the fluid pressure only (this is so Equation (12.1) may be easily solved — more general forms are allowed in the PorousFlow module).

- $\mathcal{E}_{\text{ph}}$, which is the specific internal energy of the fluid phase ph, and is measured in J.kg^{-1}, is assumed in this chapter to be

$$\mathcal{E}_{\text{ph}} = C_v^{\text{ph}} T \;, \tag{12.4}$$

where C_v^{ph} is the fluid's specific heat capacity at constant volume. This specific heat capacity is assumed constant (so that Equation (12.1) may be easily solved — more general forms are allowed in the PorousFlow module).

- λ is assumed to vary between λ^{dry} and λ^{wet}, depending on the aqueous saturation:

$$\lambda_{ij} = \lambda_{ij}^{\text{dry}} + S^n \left(\lambda_{ij}^{\text{wet}} - \lambda_{ij}^{\text{dry}} \right), \tag{12.5}$$

where S is the aqueous saturation, and n is a positive user-defined exponent. More general forms may be easily accommodated in the PorousFlow module, but to date none have been coded.

Under these conditions, Equation (12.1) becomes

$$\dot{T} = \nabla_i \alpha_{ij} \nabla_j T \;. \tag{12.6}$$

The tensor α is

$$\alpha_{ij} = \frac{\lambda_{ij}}{(1-\phi)\rho_R C_R + \rho \sum_{\text{ph}} S_{\text{ph}} \rho_{\text{ph}} C_v^{\text{ph}}} \;. \tag{12.7}$$

For constant saturation and porepressure, α_{ij} is also constant.

Consider the one-dimensional case where the spatial dimension is the semi-infinite line $x \geq 0$. Suppose that initially the temperature is constant, so that

$$T(x, t = 0) = T_0 \quad \text{for} \quad x \geq 0 \;. \tag{12.8}$$

Then apply a fixed-pressure Dirichlet boundary condition at $x = 0$ so that

$$T(x = 0, t > 0) = T_\infty \tag{12.9}$$

The solution of the above differential equation is well known to be

$$T(x, t) = T_\infty + (T_0 - T_\infty) \, \mathrm{Erf}\left(\frac{x}{\sqrt{4\alpha t}} \right), \tag{12.10}$$

where Erf is the error function.

This is verified by using the following tests on a line of 10 elements.

1. A transient analysis with no fluids. The parameters chosen are $\lambda_{ij} = \mathrm{diag}\,(2.2)$, $\phi = 0.9$, $\rho_R = 0.5$ and $C_R = 2.2$ is chosen, so that $\alpha_{ij} = 1/(0.9 \times 0.5)$.

2. A transient analysis with 2 fluid phases. The parameters chosen are $\lambda^{\text{dry}} = 0.3$, $\lambda^{\text{wet}} = 1.7$ and $S = 0.5$, so that $\lambda_{ij} = \mathrm{diag}\,(1)$. $\rho_{\text{gas}} = 0.4$, $\rho_{\text{water}} = 0.3$, $\rho_R = 0.25$, $C_v^{\text{gas}} = 1$, $C_v^{\text{water}} = 2$, $C_R = 1.0$, and $\phi = 0.8$. With these parameters, $\alpha_{ij} = 1/(0.9 \times 0.5)$.

An example verification is shown in Figure 12.1. These tests are part of the automatic test suite.
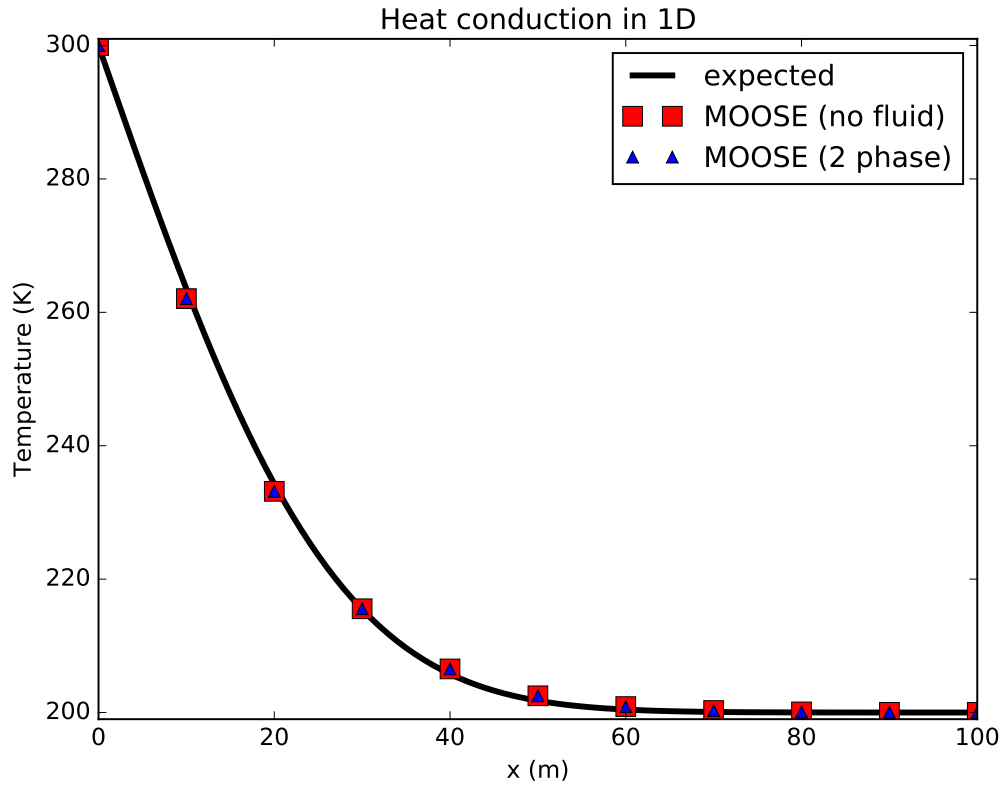
Figure 12.1: Comparison between the MOOSE result (in dots), and the exact analytic expression given by Eqn (12.10). This test had 10 elements in the x direction, with $0 \leq x \leq 100\,\mathrm{m}$, and ran for a total of 10^2 seconds with 10 timesteps.

Chapter 13

Heat advection

13.1 One-dimensional heat advection via a single-phase fluid

Consider the case of a single-phase fluid in 1 dimension, $0 \leq x \leq 1$, with the porepressure fixed at the boundaries:

$$P(x = 0, t) = 1 \quad \text{and} \quad P(x = 1, t) = 0 \ . \tag{13.1}$$

With zero gravity, and high fluid bulk modulus, the Darcy equation implies that the solution is $P(x, t) = 1 - x$, with

$$v = k/\mu \tag{13.2}$$

being the constant[1] "Darcy velocity" from $x = 0$ to $x = 1$. Here k is the porous medium's permeability, and μ is the fluid dynamic viscosity.

Suppose that the fluid internal energy is given by CT, where C is the specific heat capacity and T is its temperature. Assuming that $P/\rho \ll CT$, then the fluid's enthalpy is also CT. In this case, the energy equation reads

$$((1 - \phi)\rho_R C_R + \phi\rho C) \frac{\partial T}{\partial t} + C\rho v \frac{\partial T}{\partial x} = 0 \ . \tag{13.3}$$

This is the wave equation with velocity

$$v_T = \frac{C\rho v}{(1 - \phi)\rho_R C_R + \phi\rho C} \ . \tag{13.4}$$

Recall that the "Darcy velocity" is $v = k/\mu$.

Let the initial condition for T be $T(x, t = 0) = 200$. Apply the boundary conditions

$$T(x = 0, t) = 300 \quad \text{and} \quad T(x = 1, t) = 200 \ . \tag{13.5}$$

---

[1]To get the velocity of the individual fluid particles, this should be divided by the porosity.

At $t = 0$ this creates a front at $x = 0$. Choose the parameters $C = 2$, $C_R = 1$, $\rho = 1000$, $\rho_R = 125$, $\phi = 0.2$, $k = 1.1$, $\mu = 4.4$ (all in consistent units), so that $v_T = 1$ is the front's velocity.

The sharp front is *not* maintained by MOOSE. This is due to numerical diffusion, which is particularly strong in the upwinding scheme implemented in the PorousFlow module. Nevertheless, MOOSE advects the smooth front with the correct velocity, as shown in Figure 13.1.

The sharp front is *not* maintained by MOOSE even when no upwinding is used. In the case at hand, which uses a fully-saturated single-phase fluid, the `FullySaturated` versions of the Kernels may be used in order to compare with the standard fully-upwinded Kernels. The `FullySaturated` Kernels do not employ any upwinding whatsoever, so less numerical diffusion is expected. This is demonstrated in Figure 13.1. Two additional points may also be nocied: (1) the lack of upwinding has produced a "bump" in the temperature profile near the hotter side; (2) the lack of upwinding means the temperature profile moves slightly slower than it should. These two affects reduce as the mesh density is increased, however.
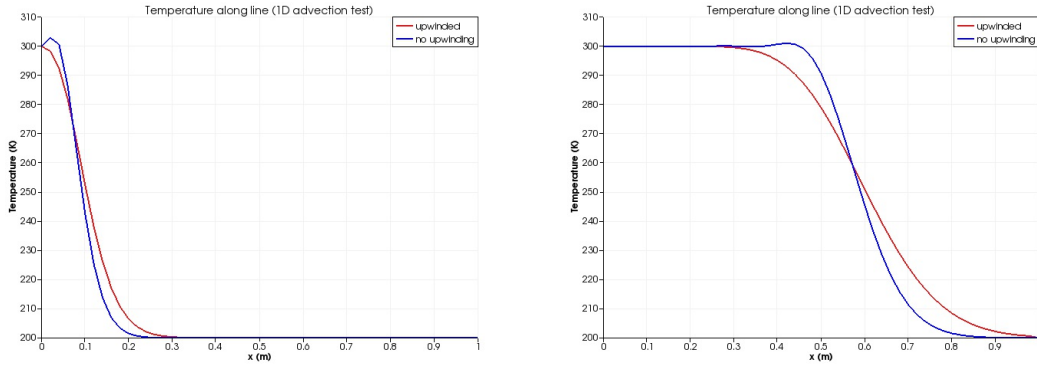

Figure 13.1: Results of heat advection via a fluid in 1D. The fluid flows with constant Darcy velocity of $0.25\,\mathrm{m.s}^{-1}$ to the right, and this advects a temperature front at velocity $1\,\mathrm{m.s}^{-1}$ to the right. The pictures above that the numerical implementation of porous flow within MOOSE (including upwinding) diffuses sharp fronts, but advects them at the correct velocity (notice the centre of the upwinded front is at the correct position in each picture). Less diffusion is experienced without upwinding. Left: temperature $t = 0.1\,\mathrm{s}$. Right: temperature at $t = 0.6\,\mathrm{s}$.

Chapter 14

Newton cooling

14.1 Classic Newton cooling in a bar

Without fluids, mechanical deformation and sinks, the heat equation is

$$\rho_R C_R (1 - \phi)\dot{T} = \nabla \lambda \nabla T \ , \tag{14.1}$$

where ϕ is the porosity, ρ_R is the rock grain density (kg.m^{-3}), C_R is the rock grain specific heat capacity (J.kg^{-1}.K^{-1}), T is the temperature, and λ is the tensorial thermal conductivity of the porous material (J.s^{-1}.K^{-1}.m^{-1}).

In section 14.2, the dynamics of this equation is explored, while this section concentrates on the steady-state situation. Consider the one-dimensional case where a bar sits between $x = 0$ and $x = L$ with a fixed temperature at $x = 0$:

$$T(x = 0, t) = T_0 \ , \tag{14.2}$$

and a sink flux at the other end:

$$\text{sink strength (J.m}^{-2}.\text{s}^{-1}) = \lambda \frac{\partial T}{\partial x}\bigg|_{x=L} = -C\left(T - T_e\right)_{x=L} \ . \tag{14.3}$$

Here T_e is a fixed quantity ("e" stands for "external"), and C is a constant conductance (J.m^{-2}.s^{-1}.K^{-1}).

The solution is the linear function

$$T = T_0 + \frac{T_e - T_0}{\lambda + CL}Cx \ . \tag{14.4}$$

The heat sink in Eqn (14.3) is a linear function of T, so the `PorousFlowPiecewiseLinearSink` may be employed.

The simulation is run in MOOSE using $C = 1$, $L = 100$, $\lambda = 100$, $T_0 = 2$ and $T_e = 1$. The solution is shown in Figure 14.1
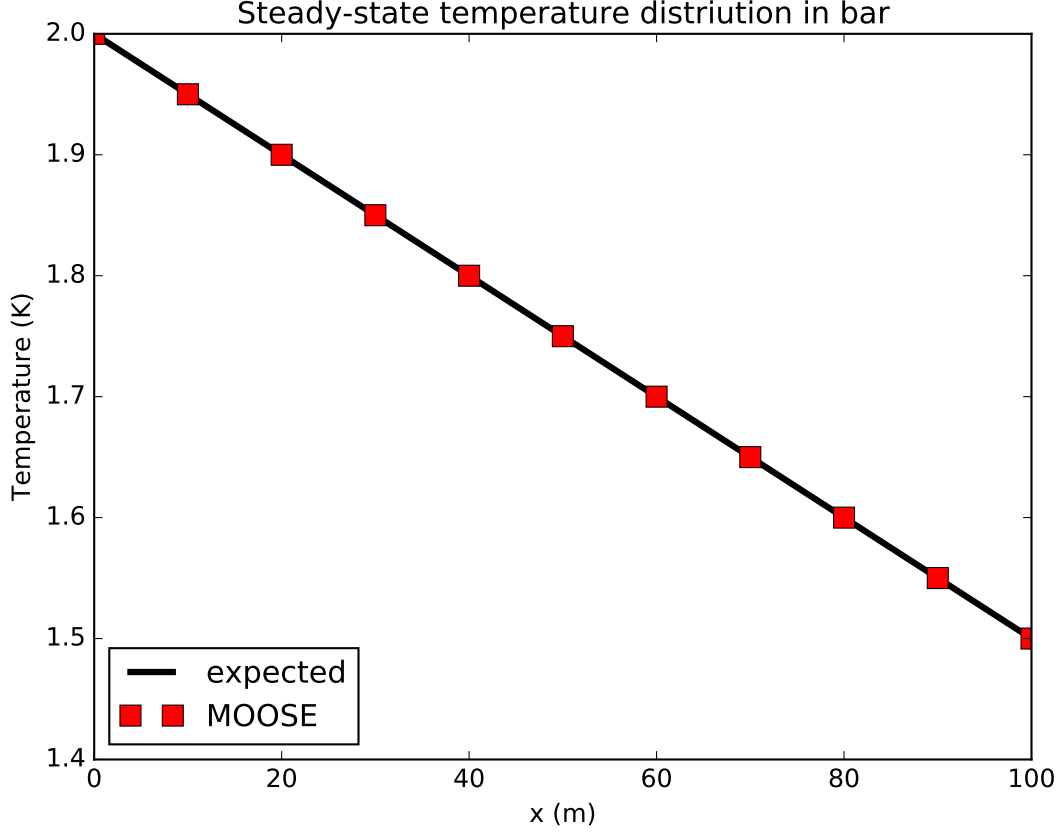
Figure 14.1: The steady-state temperature in the bar. MOOSE agrees well with theory illustrating that piecewise-linear heat sinks/sources and heat conduction are correctly implemented in MOOSE.

14.2 Porepressure sink in a bar

These tests demonstrate that MOOSE behaves correctly when a simulation contains a sink. The sink is a piecewise linear function of pressure.

Darcy's equation for (single-phase) flow through a fully saturated medium without gravity and without sources is

$$\frac{\partial}{\partial t}\phi\rho = \nabla_i \left(\frac{\rho\kappa_{ij}}{\mu}\nabla_j P \right) \ , \tag{14.5}$$

with the following notation:

- ϕ is the medium's porosity;

- ρ is the fluid density;

- κ_{ij} is the permeability tensor;

- μ is the fluid viscosity;

- $\partial/\partial t$ and ∇_i denote the time and spatial derivatives, respectively.

Using $\rho \propto \exp(P/B)$, where B is the fluid bulk modulus, Darcy's equation becomes

$$\frac{\partial}{\partial t}\rho = \nabla_i \alpha_{ij} \nabla_j \rho \ , \tag{14.6}$$

with

$$\alpha_{ij} = \frac{\kappa_{ij} B}{\mu \phi} \ . \tag{14.7}$$

Here the porosity and bulk modulus are assumed to be constant in space and time.

Consider the one-dimensional case where a bar sits between $x = 0$ and $x = L$ with initial pressure distribution so $\rho(x, t = 0) = \rho_0(x)$. Maintain the end $x = 0$ at constant pressure, so that $\rho(x = 0, t) = \rho_0(0)$. At the end $x = L$, prescribe a sink flux

$$\left.\frac{\partial \rho}{\partial x}\right|_{x=L} = -C\left(\rho - \rho_e\right)_{x=L} \ , \tag{14.8}$$

where ρ_e is a fixed quantity ("e" stands for "external"), and C is a constant conductance. This corresponds to the flux

$$\left.\frac{\partial P}{\partial x}\right|_{x=L} = -CB\left(1 - e^{(P_e - P)/B}\right)_{x=L} \ , \tag{14.9}$$

which can easily be coded into a MOOSE input file: the flux is $\rho \kappa \nabla P / \mu = -CB\kappa(e^{P/B} - e^{P_e/B})/\mu$, and this may be represented by a piecewise linear function of pressure.

The solution of this problem is well known and is

$$\rho(x, t) = \rho_0(0) - \frac{\rho_0(0) - \rho_e}{1 + LC}Cx + \sum_{n=1}^{\infty} a_n \sin\frac{k_n x}{L} e^{-k_n^2 \alpha t/L^2} \ , \tag{14.10}$$

where k_n is the nth positive root of the equation $LC \tan k + k = 0$ (k_n is a little bigger than $(2n - 1)\pi/2$), and a_n is determined from

$$a_n \int_0^L \sin^2\frac{k_n x}{L} \, dx = \int_0^L \left(\rho_0(x) - \rho_0(0) + \frac{\rho_0(0) - \rho_e}{1 + LC}Cx\right) \sin\frac{k_n x}{L} \, dx \ , \tag{14.11}$$

which may be solved numerically (Mathematica is used to generate the solution in Figure 14.2).

The problem is solved in MOOSE using the following parameters:

Bar length	$100\,\mathrm{m}$
Bar porosity	0.1
Bar permeability	$10^{-15}\,\mathrm{m^2}$
Gravity	0
Water density	$1000\,\mathrm{kg.m^{-3}}$
Water viscosity	$0.001\,\mathrm{Pa.s}$
Water bulk modulus	$1\,\mathrm{MPa}$
Initial porepressure P_0	$2\,\mathrm{MPa}$
Environmental pressure P_e	0
Conductance C	$0.05389\,\mathrm{m^{-1}}$

This conductance is chosen so at steadystate $\rho(x = L) = 2000\,\mathrm{kg.m^{-3}}$.

The problem is solved using 1000 elements along the x direction ($L = 100\,\mathrm{m}$), and using 100 time-steps of size $10^6\,\mathrm{s}$. Using fewer elements or fewer timesteps means the agreement with the theory is marginally poorer. Two tests are performed: one with transient flow, and one using the steadystate solver. In this case the initial condition is $P = 2 - x/L\,\mathrm{MPa}$, since the uniform $P = 2\,\mathrm{MPa}$ does not converge. The results are shown in Figure 14.2.

14.3 Porepressure sink in a bar with heat

The simulation of Section 14.2 is re-run, but this time heat flow is included. In this section it is assumed that the fluid specific enthalpy $(\mathrm{J.kg^{-1}})$ is exactly equal to the fluid internal energy, and that internal energy is ideal:

$$h = \mathcal{E} = C_v T \ . \tag{14.12}$$

This makes the arguments below simple without having to consider real fluids with complicated enthalpy and density expressions.

At the left end of the bar, the temperature is kept fixed:

$$T(x = 0, t) = T_0 \ . \tag{14.13}$$

At the other end of the bar, heat is removed only by the fluid flowing out of the system. That is, there is a heat sink:

$$\text{sink strength } (\mathrm{J.m^{-2}.s^{-1}}) = -C\mathcal{E}\,(\rho - \rho_e)_{x=L} \ . \tag{14.14}$$

No other sinks or sources are applied to the heat equation.

With this setup, the steady-state temperature in the bar must be exactly

$$T(x, t = \infty) = T_0 \ . \tag{14.15}$$

For consider the fluid flowing from $x = 0$ to $x = L$ in order to assume steady-state. At $x = 0$ it must have temperature T_0 because that temperature is fixed at $x = 0$. It advects
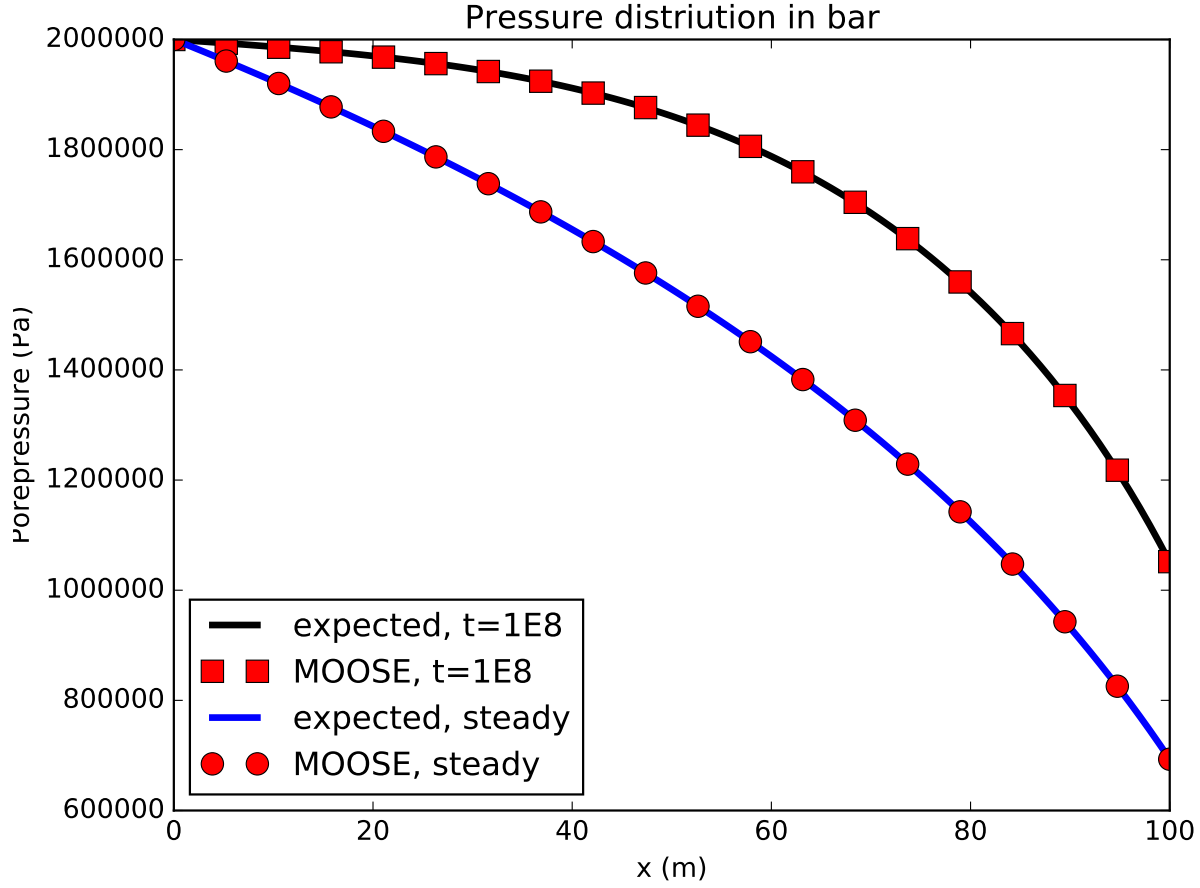
Figure 14.2: The porepressure in the bar at $t = 10^8$ s, and at steadystate. The pressure at $x = 0$ is held fixed, while the sink is applied at $x = 100$ m. MOOSE agrees well with theory demonstrating that piecewise-linear sinks/sources and single-phase Darcy fluid flow are correctly implemented in MOOSE.

this temperature with it as it moves, so therefore at $t = \infty$, this temperature has permeated throughout the entire bar. This occurs even without heat conduction, and is independent of the initial temperature of the bar.

MOOSE produces this result exactly.

Chapter 15

Hot ideal fluid in a bar

This test uses a similar setup to Section 14.3, except that here an ideal fluid is used. The use of an ideal gas simplifies the equations. Only the steady-state is studied in this section.

The governing equation for the fluid's porepressure P is

$$\nabla \frac{\rho \kappa}{\mu} \nabla P = 0 \ . \tag{15.1}$$

It is assumed that κ and μ are constant, and that

$$\rho = \frac{MP}{RT} \ , \tag{15.2}$$

holds (this is the ideal gas equation of state). In this formula M is the gas molar mass, R is the gas constant and T is the temperature.

The equation governing the temperature is assumed to be just the fluid advection equation

$$\nabla \frac{h \rho \kappa}{\mu} \nabla P = 0 \ . \tag{15.3}$$

As in Section 14.3, heat conduction could be added, but it is actually irrelevant since the solution to the problem below is constant T. The enthalpy, h, for an ideal gas is

$$h = C_v T + \frac{P}{\rho} = C_v T + \frac{RT}{M} = C_p T \ . \tag{15.4}$$

The boundary conditions at the left-hand end are

$$P(x = 0) = P_0 \quad \text{and} \quad T(x = 0) = T_0 \ . \tag{15.5}$$

Physically these correspond to fluid and heat being removed or added to the left-hand end by some external source in order to keep the porepressure and temperature fixed.

The porepressure boundary condition at the right-hand end of the bar is

$$\text{sink flux } (\text{kg.m}^{-2}.\text{s}^{-1}) = \left.\frac{\rho\kappa}{\mu}\nabla P\right|_{x=L} = \left.-C\frac{\rho\kappa}{\mu}(P - P_e)\right|_{x=L} . \tag{15.6}$$

Physically this corresponds to the mass-flow through the boundary being proportional to $P - P_e$. Here P_e is a fixed "environmental" porepressure, and this acts as a source or sink of fluid. C is the "conductance" of the boundary. Notice the appearence of $\rho\kappa/\mu$ in the LHS of this equation means that this is truly a flux of fluid mass (measured in kg.m^{-2}.s^{-1}), and the appearence of $\rho\kappa/\mu$ on the RHS means that a `PorousFlowPiecewiseLinearFlux` may be used with `use_mobility=true`.

The temperature boundary condition at the right-hand end of the bar is

$$\text{heat flux } (\text{J.m}^{-2}.\text{s}^{-1}) = \left.\frac{h\rho\kappa}{\mu}\nabla P\right|_{x=L} = \left.-C\frac{h\rho\kappa}{\mu}(P - P_e)\right|_{x=L} . \tag{15.7}$$

Comparing this with Equation 15.6, it is seen that this is exactly the heat loss (or gain) at the boundary corresponding to the loss (or gain) of the fluid. Notice the appearence of $h\rho\kappa/\mu$ in the LHS of this equation means that this is truly a flux of fluid mass (measured in J.m^{-2}.s^{-1}), and the appearence of $h\rho\kappa/\mu$ on the RHS means that a `PorousFlowPiecewiseLinearFlux` may be used with `use_mobility=true` and `use_enthalpy=true`.

There is a clear similarity between the fluid and heat equations. The heat equation does not actually depend on temperature, and is simply

$$0 = \nabla(P\nabla P) , \tag{15.8}$$

which is solved by

$$P^2 = P_0^2 + Ax . \tag{15.9}$$

The fluid equation then yields

$$T(x) = T_0 . \tag{15.10}$$

The constant A may be determined from the either of the boundary conditions. For the special case of $P_e = 0$ and $2LC = 1$, the solution is

$$P = P_0\sqrt{1 - \frac{x}{2L}} . \tag{15.11}$$

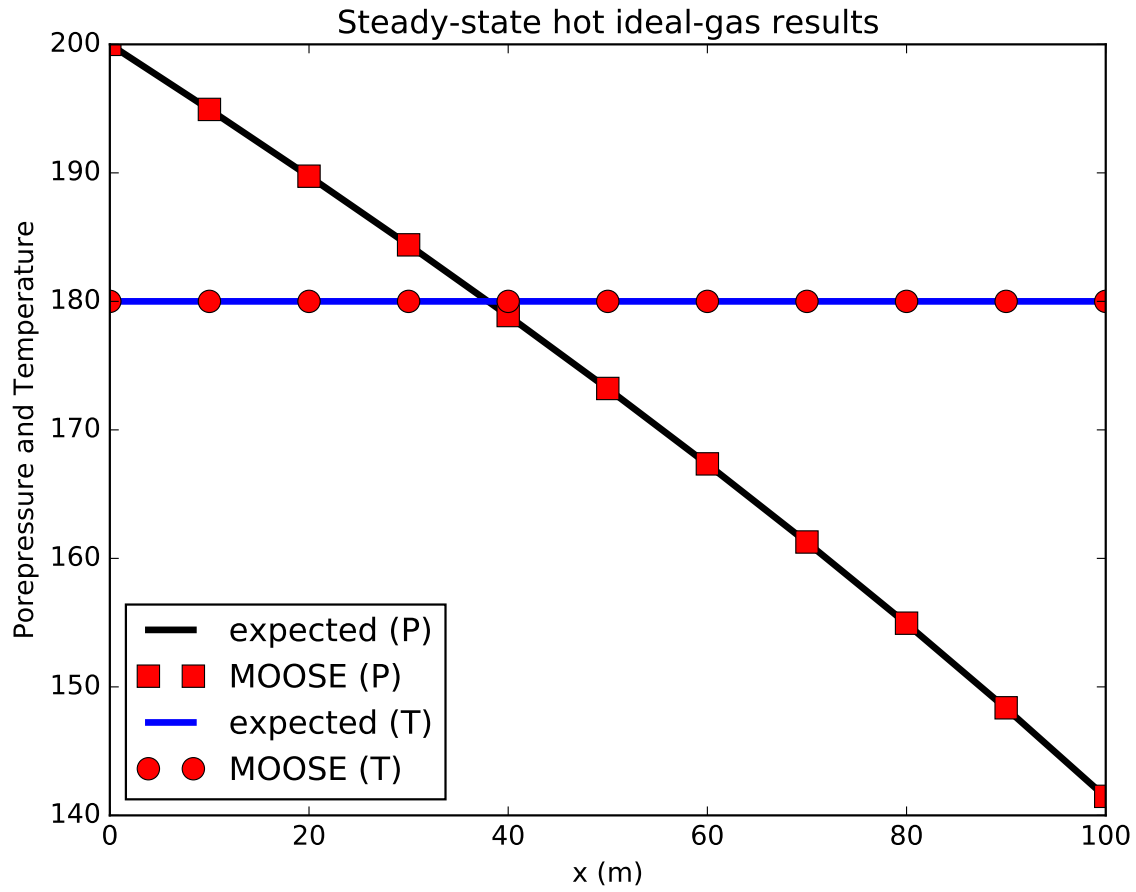MOOSE produces this result exactly, as illustrated in Figure 15.1

Figure 15.1: The steady-state porepressure and temperature distributions in the bar ($P_0 = 200$ and $T_0 = 180$). MOOSE agrees well with theory illustrating that piecewise-linear fluid and heat sinks/sources as well as ideal fluids are correctly implemented in MOOSE.

Chapter 16

Poroelasticitiy

16.1   Introduction

The PorousFlow module includes the ability to couple fluid flow to solid mechanics, and thus includes poroelasticity, which is the theory of a fully-saturated single-phase fluid with constant bulk density and constant viscosity coupled to small-strain isotropic elasticity.

There is one important difference between the theories, however. The time-derivative terms of poroelasticity are

$$\frac{1}{M}\dot{P} + \alpha\dot{\epsilon}_{ii} \ , \tag{16.1}$$

where M is the Biot modulus:

$$\frac{1}{M} = \frac{(1-\alpha)(\alpha-\phi)}{K} + \frac{\phi}{K_{\mathrm{f}}} \ , \tag{16.2}$$

P is the fluid porepressure, α is the Biot coefficient, ϵ_{ii} is the volumetric strain, ϕ is the porosity, K is the solid (drained) bulk modulus, and K_{f} is the fluid bulk modulus. Evidently from Eqn (16.2), the Biot modulus, M, should evolve with time as the porosity evolves. Indeed, the terms in Eqn (16.1) are derived from the continuity equation $\partial(\phi\rho)/\partial t + \phi\rho\dot{\epsilon}_{ii}$ using the evolution of ϕ (and that $\rho = \rho_0 \exp(P/K_{\mathrm{f}})$). However, in the standard analytical solutions of poroelasticity theory, the Biot modulus, M is considered fixed.

The PorousFlow module allows porosity to vary with fluid porepressure and volumetric strain, so usually the Biot modulus would vary too, causing differences with the analytical solutions of poroelasticity. Therefore, PorousFlow offers a porosity relationship that evolves porosity in such a way as to keep M fixed. This is called `PorousFlowPorosityHMBiotModulus`.

PorousFlow is also built with finite strains in mind, whereas poroelasticity is not. Therefore, in comparisons with solutions from poroelasticity theory, either the strain should be kept small, or the various finite-strain switches in PorousFlow should be turned off (they are all on by default).

16.2 Volumetric expansion due to increasing porepressure

The porepressure within a fully-saturated sample is increased:

$$P_{\mathrm{f}} = t \ . \tag{16.3}$$

Zero mechanical pressure is applied to the sample's exterior, so that no Neumann BCs are needed on the sample. No fluid flow occurs since the porepressure is increased uniformly throughout the sample

The effective stresses should then evolve as $\sigma_{ij}^{\mathrm{eff}} = \alpha t \delta_{ij}$, and the volumetric strain $\epsilon_{00} + \epsilon_{11} + \epsilon_{22} = \alpha t / K$. MOOSE produces this result correctly.

16.3 Undrained oedometer test

A cubic single-element fully-saturated sample has roller BCs applied to its sides and bottom. All the sample's boundaries are impermeable. A downwards (normal) displacement, u_z, is applied to its top, and the rise in porepressure and effective stress is observed. (Here z denotes the direction normal to the top face.) There is no fluid flow in the single element.

Under these conditions, assuming constant porosity, and denoting the height (z length) of the sample by L:

$$
\begin{aligned}
P_{\mathrm{f}} &= -K_f \log(1 - u_z) \ , \\
\sigma_{xx}^{\mathrm{eff}} &= (K - \tfrac{2}{3}G)u_z/L \ , \\
\sigma_{zz}^{\mathrm{eff}} &= (K + \tfrac{4}{3}G)u_z/L \ .
\end{aligned}
\tag{16.4}
$$

16.4 Porepressure generation of a confined sample

A single-element fully-saturated sample is constrained on all sides and its boundaries are impermeable. Fluid is pumped into the sample via a source s (kg.s^{-1}.m^{-3}) and the rise in porepressure is observed.

Denoting the strength of the source by s (units are s^{-1}), the expected result is

$$
\begin{aligned}
\text{fluid mass} &= \text{fluid mass}_0 + st \ , \\
\sigma_{ij}^{\mathrm{eff}} &= 0 \ , \\
P_{\mathrm{f}} &= K_{\mathrm{f}} \log(\rho\phi/\rho_0) \ , \\
\rho &= \rho_0 \exp(P_{\mathrm{f}}/K_f) \ , \\
\phi &= \alpha + (\phi_0 - \alpha) \exp\left(P_{\mathrm{f}}(\alpha - 1)/K\right) \ .
\end{aligned}
\tag{16.5}
$$

$$\tag{16.6}$$

Here K is the solid bulk modulus.

16.5   Porepressure generation of an unconfined sample

A single-element fully-saturated sample is constrained on all sides, except its top. All its boundaries are impermeable. Fluid is pumped into the sample via a source s (kg.s^{-1}.m^{-3})) and the rise in the top surface, the porepressure, and the stress are observed.

Regardless of the evolution of porosity, the following ratios result

$$
\begin{aligned}
\sigma_{xx}/\epsilon_{zz} &= K - 2G/3 \ , \\
\sigma_{zz}/\epsilon_{zz} &= K + 4G/3 \ , \\
P/\epsilon_{zz} &= (K + 3G/3 + \alpha^2 M)/\alpha - \alpha M \ .
\end{aligned}
\tag{16.7}
$$

where K is the undrained bulk modulus, G the shear modulus, α the Biot coefficient, and M is the initial Biot modulus. MOOSE produces these results when using the `PorousFlowPorosityHM` material.

However, if the Biot modulus, M, is held fixed as the porosity evolves, and the source is

$$
s = S\rho_0 \exp(P/K_{\mathrm{f}}) \ ,
\tag{16.8}
$$

with S being a *constant* volumetric source (m^3.s^{-1}.m^{-3}) then

$$
\begin{aligned}
\epsilon_{zz} &= \frac{\alpha M s t}{K + 4G/3 + \alpha^2 M} \ , \\
P &= M(st - \alpha \epsilon_{zz}) \ , \\
\sigma_{xx} &= (K - 2G/3)\epsilon_{zz} \ , \\
\sigma_{zz} &= (K + 4G/3)\epsilon_{zz} \ .
\end{aligned}
\tag{16.9}
$$

MOOSE produces these results when using the `PorousFlowPorosityHMBiotModulus` material.

16.6   Terzaghi consolidation

This is documented at `http://mooseframework.org/wiki/PhysicsModules/TensorMechanics/TensorMech`
The PorousFlow Material `PorousFlowPorosityHMBiotModulus` must be used.

16.7   Mandel's consolidation of a drained medium

A sample's dimensions are $-a \le x \le a$ and $-b \le y \le b$, and it is in plane strain (no z displacement). It is squashed with constant normal force by impermeable, frictionless plattens

on its top and bottom surfaces (at $y = \pm b$). Fluid is allowed to leak out from its sides (at $x = \pm a$), but all other surfaces are impermeable. This is called Mandel's problem and it is shown graphically in Fig 16.1
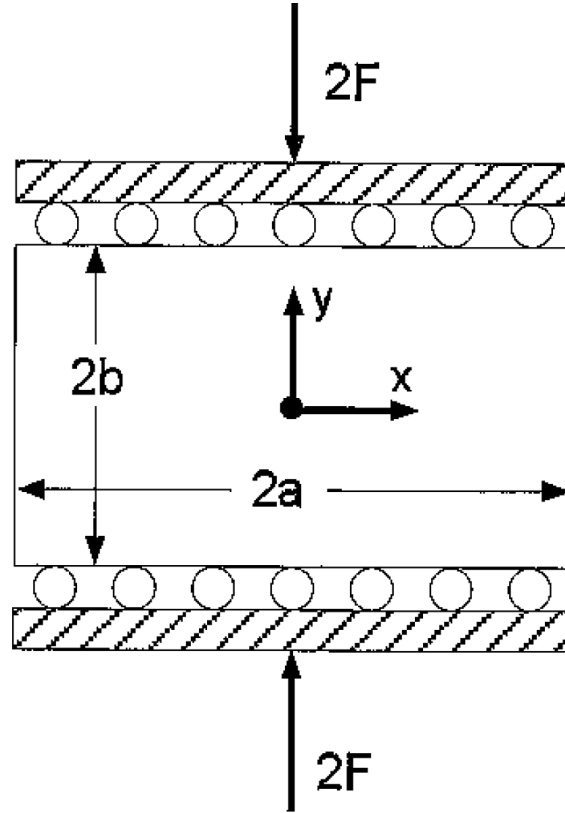

Figure 16.1: The setup of the Mandel experiment: a force F squashes a porous material with impermeable plattens. This causes fluid to seep from the material.

The interesting feature of this problem (apart from that it can be solved analytically) is that the porepressure in the sample's center actually increases for a short time after application of the force. This is because the leakage of the fluid from the sample's sides causes an apparent softening of the material near those sides. This means stress concentrates towards the sample's center which causes an increase in porepressure. Of course, eventually the fluid totally drains from the sample, and the porepressure is zero. As the fluid drains from the sample's sides the plattens move slowly towards each other.

The solution for porepressure and displacements is given in: AHD Cheng and E Detournay "A direct boundary element method for plane strain poroelasticity" International Journal of Numerical and Analytical Methods in Geomechanics 12 (1988) 551-572. The solution involves rather lengthy infinite series, so I will not write it here.

As is common in the literature, this is simulated by considering the quarter-sample, $0 \le x \le a$ and $0 \le y \le b$, with impermeable, roller BCs at $x = 0$ and $y = 0$ and $y = b$. Porepressure is fixed at zero on $x = a$. Porepressure and displacement are initialised to zero. Then the top ($y = b$) is moved downwards with prescribed velocity, so that the total force that is induced

by this downwards velocity is fixed. The velocity is worked out by solving Mandel's problem analytically, and the total force is monitored in the simulation to check that it indeed remains constant.

The simulations in the PorousFlow test suite use 10 elements in the x direction and 1 in the y direction. Four types of simulation are run:

1. HM. This uses standard PorousFlow Materials and Kernels, in particular it uses the "HM" porosity relationship. This is not expected to agree perfectly with the analytical solutions because: the solutions assume constant Biot modulus.

2. constM. This is identical to the HM case, save that it uses a porosity evolution law that keeps the Biot modulus fixed. It is therefore expected to agree with the analytical solutions.

3. FullSat. This uses the FullySaturated versions of the fluid mass time derivative and the fluid flux. In this case the Biot modulus is kept fixed, so it is expected to agree with the analytical solutions.

4. FullSatVol. This uses the FullySaturated versions of the fluid mass time derivative and the fluid flux, and does not multiply by the fluid density. Therefore this version is identical to what is usually implemented in poro-elastic codes. It is linear and therefore converges in only one iteration. In this case the Biot modulus is kept fixed, so it is expected to agree with the analytical solutions.

Of course there are minor discrepancies between the last three and the analytical solution that are brought about through spatial and temporal discretisation errors. The figures below present the results.
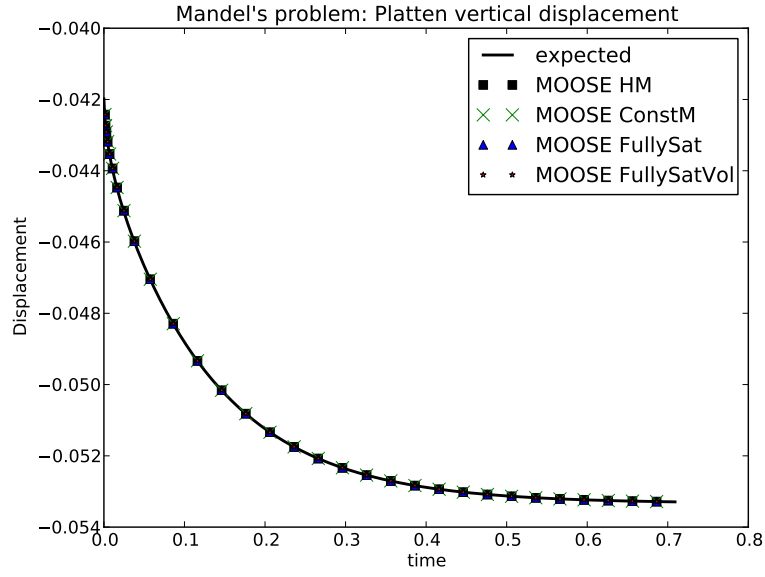
Figure 16.2: The vertical displacement of the platten as a function of time.
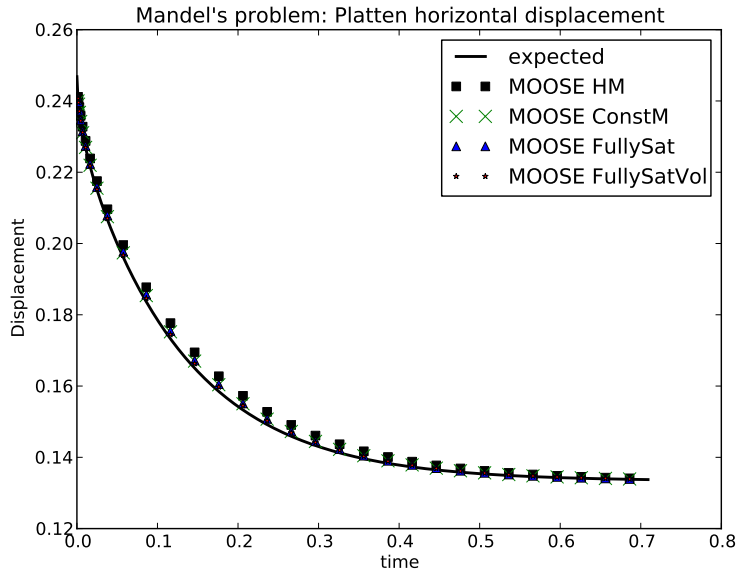

Figure 16.3: The horizontal displacement of the material at $(x, y) = (a, b)$ as a function of time.
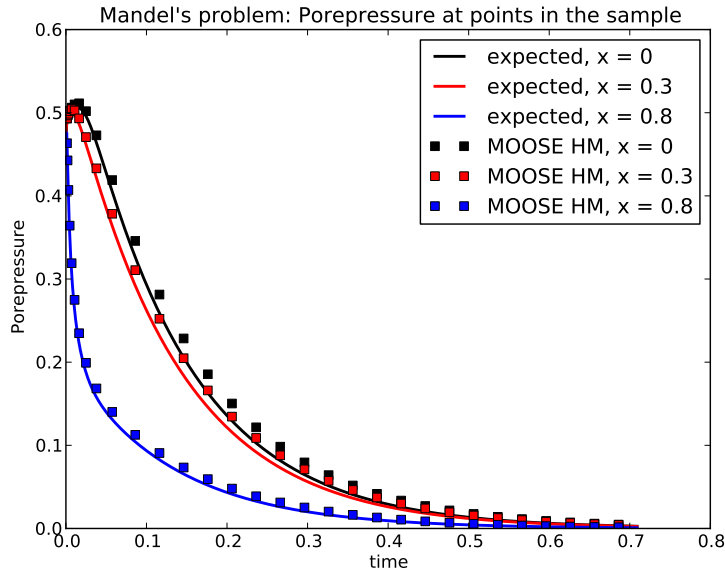
Figure 16.4: The porepressure at various points in the sample in the HM model with $a = 1$.
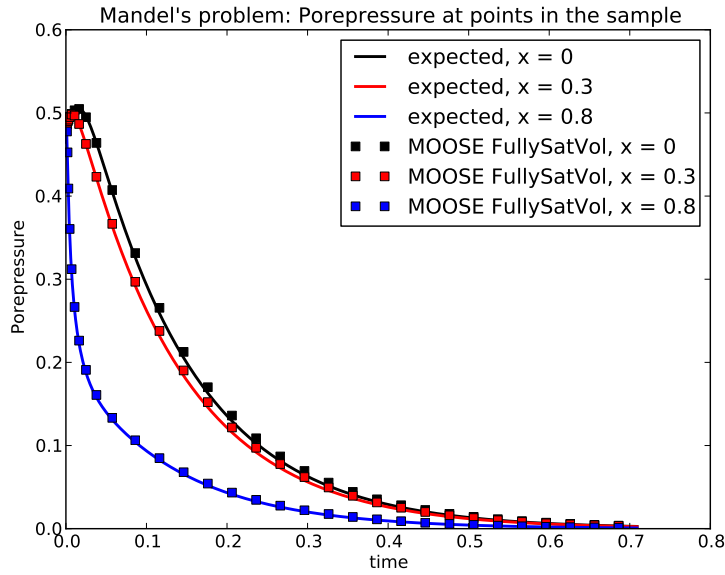

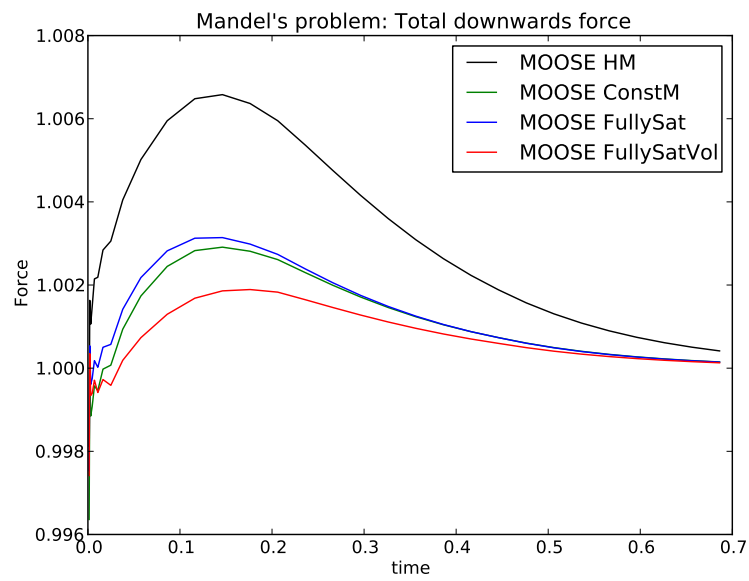Figure 16.5: The porepressure at various points in the sample in the FullSatVol model with $a = 1$.

Figure 16.6: The total downwards force on the platten as a function of time. This should be unity.

Chapter 17

Plastic Heat

17.1 Plastic deformation heating a porous skeleton

In this section, plastic deformation causes a heat energy-density rate $(\text{J.m}^{-3}.\text{s}^{-1})$ of

$$c(1 - \phi)\sigma_{ij}\epsilon_{ij}^{\text{plastic}} , \tag{17.1}$$

where c is a coefficient (s^{-1}), ϕ is the porosity, σ is the stress, and $\epsilon^{\text{plastic}}$ is the plastic strain.

There is no fluid, and no heat flow is studied: the heat energy released simply heats up the porous skeleton:

$$\frac{\partial}{\partial t}(1 - \phi)c_R\rho_R T = c(1 - \phi)\sigma_{ij}\epsilon_{ij}^{\text{plastic}} . \tag{17.2}$$

The porosity (ϕ) and volumetric heat capacity of the rock grains $(c_R\rho_R)$ are chosen to be constant.

Perfect capped weak-plane plasticity is used, so that the admissible zone is defined by

$$\sigma_{zz} \leq S_T , \tag{17.3}$$
$$\sigma_{zz} \geq -S_C \tag{17.4}$$
$$\sqrt{\sigma_{zx}^2 + \sigma_{zy}^2} + \sigma_{zz}\tan\Phi \leq C . \tag{17.5}$$

Here S_T is the tensile strength, S_C is the compressive strength, C is the cohesion and Φ is the friction angle. The elastic tensor is chosen to be

$$E_{ijkl} = \lambda\delta_{ij}\delta_{kl} + \mu(\delta_{ik}\delta_{jl} + \delta_{il}\delta_{jk}) . \tag{17.6}$$

The parameters in these expressions are chosen to be: $S_T = 1$, $S_C = 1$, $C = 1$, $\Phi = \pi/4$, $\lambda = 1/2$, and $\mu = 1/4$ (all in consistent units).

In each experiment a single finite-element is used.

17.2 Tensile failure

The top of the finite element is pulled upwards with displacement:

$$u_z = zt \ , \tag{17.7}$$

while the displacement in the x and y directions is chosen to be zero. This implies the only non-zero component of total strain is

$$\epsilon_{zz}^{\text{total}} = t \ . \tag{17.8}$$

The constitutive law implies

$$\sigma_{zz} = t \ . \tag{17.9}$$

This stress is admissible for $t \leq 1$, while for $t > 1$ the system yields in tension:

$$\sigma_{zz} = 1 \quad \text{for } t > 1 \ , \tag{17.10}$$

and the plastic strain is,

$$\epsilon_{zz}^{\text{plastic}} = t - 1 \quad \text{for } t > 1 \ . \tag{17.11}$$

This means that the material's temperature should increase as

$$c_R \rho_R \dot{T} = c \quad \text{for } t > 1 \ , \tag{17.12}$$

while the right-hand side is zero for $t \leq 1$.

17.3 Compressive failure

The top of the finite element is pushed downwards with displacement:

$$u_z = -zt \ , \tag{17.13}$$

while the displacement in the x and y directions is chosen to be zero. This implies only non-zero component of total strain is

$$\epsilon_{zz}^{\text{total}} = -t \ . \tag{17.14}$$

The constitutive law implies

$$\sigma_{zz} = -t \ . \tag{17.15}$$

This stress is admissible for $t \leq 1$, while for $t > 1$ the system yields in compression

$$\sigma_{zz} = -1 \quad \text{for } t > 1 \ , \tag{17.16}$$

and the plastic strain is,

$$\epsilon_{zz}^{\text{plastic}} = -(t - 1) \quad \text{for } t > 1 \ . \tag{17.17}$$

This means that the material's temperature should increase as

$$c_R \rho_R \dot{T} = c \quad \text{for } t > 1 \ , \tag{17.18}$$

while the right-hand side is zero for $t \leq 1$.

17.4   Shear failure

The top of the finite element is sheared with displacement:

$$u_x = zt \;, \tag{17.19}$$

while the displacement in the y and z directions is chosen to be zero. This implies only non-zero component of total strain is

$$\epsilon_{xz}^{\text{total}} = t \;. \tag{17.20}$$

The constitutive law implies

$$\sigma_{xz} = t/4 \;. \tag{17.21}$$

This stress is admissible for $t \leq 4$, while for $t > 4$ the system yields in shear:

$$\sigma_{xz} = 1 \quad \text{for } t > 4 \;, \tag{17.22}$$

and the plastic strain is,

$$\epsilon_{xz}^{\text{plastic}} = t - 4 \quad \text{for } t > 4 \;. \tag{17.23}$$

This means that the material's temperature should increase as

$$c_R \rho_R \dot{T} = c \quad \text{for } t > 4 \;, \tag{17.24}$$

while the right-hand side is zero for $t \leq 4$.